HHS Public Access

Author manuscript

Cell Rep. Author manuscript; available in PMC 2023 May 29.

Published in final edited form as:

Cell Rep. 2022 September 13; 40(11): 111341. doi:10.1016/j.celrep.2022.111341.

Gut commensal bacteria enhance pathogenesis of a tumorigenic murine retrovirus

Jessica Spring[1], **Aly A. Khan**[2], **Sophie Lara**[3], **Kelly O'Grady**[3], **Jessica Wilks**[1], **Sandeep Gurbuxani**[2], **Steven Erickson**[4], **Michael Fischbach**[5], **Amy Jacobson**[5], **Alexander Chervonsky**[1,2,4], **Tatyana Golovkina**[1,3,4,6,7,*]

[1]Committee on Microbiology, University of Chicago, Chicago, IL 60637, USA

[2]Department of Pathology, University of Chicago, Chicago, IL 60637, USA

[3]Department of Microbiology, University of Chicago, Chicago, IL 60637, USA

[4]Committee on Immunology, University of Chicago, Chicago, IL 60637, USA

[5]Department of Bioengineering, Stanford University, Stanford, CA 94305, USA

[6]Committee on Genetics, Genomics and System Biology, University of Chicago, Chicago, IL 60637, USA

[7]Lead contact

SUMMARY

The influence of the microbiota on viral transmission and replication is well appreciated. However, its impact on retroviral pathogenesis outside of transmission/replication control remains unknown. Using murine leukemia virus (MuLV), we found that some commensal bacteria promoted the development of leukemia induced by this retrovirus. The promotion of leukemia development by commensals is due to suppression of the adaptive immune response through upregulation of several negative regulators of immunity. These negative regulators include Serpinb9b and Rnf128, which are associated with a poor prognosis of some spontaneous human cancers. Upregulation of Serpinb9b is mediated by sensing of bacteria by the NOD1/NOD2/RIPK2 pathway. This work describes a mechanism by which the microbiota enhances tumorigenesis within gut-distant organs and points at potential targets for cancer therapy.

*Correspondence: tgolovki@bsd.uchicago.edu.

AUTHOR CONTRIBUTIONS

J.S. performed most of the experiments reported in the paper. A.A.K. carried out computational analysis of the RNA-seq data. K.O'G. performed experiments with IL-6- and RAG1-deficient mice. J.W. conducted experiments with Abx-treated mice, experiments on erythroid differentiation, and monitored ASF-colonized mice. S.L. performed real time PCRs and IC assays for Serpinb9b$^{-/-}$ and Rnf128$^{-/-}$ mice. S.G. generated the leukemia scoring system, scored splenic tissue sections, and contributed to experimental design. S.E. helped to design CRISPR-Cas9 approaches to target Serpinb9b and Rnf128. A.J. cultivated *B. thetaiotaomicron*. M.F. and A.C. contributed to experimental design and the edit of the manuscript. J.S. and T.G. wrote the manuscript. T.G. conceived the project and performed many of the experiments.

SUPPLEMENTAL INFORMATION

Supplemental information can be found online at https://doi.org/10.1016/j.celrep.2022.111341.

DECLARATION OF INTERESTS

The authors declare no competing interests.

Graphical abstract

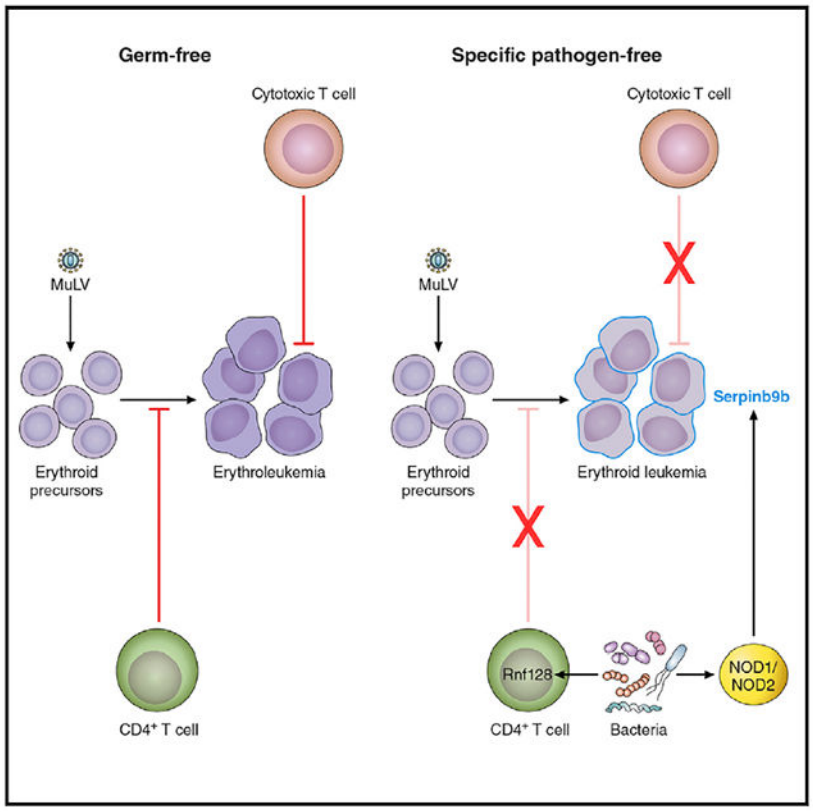

In brief

Spring et al. show that commensal bacteria promote the development of virally induced leukemia through suppression of the adaptive immune response. Suppression is mediated by the upregulation of negative immune regulators and by drivers of tumorigenesis, Rnf128 and Serpinb9b.

INTRODUCTION

The commensal microbiota plays a critical role in maintaining host health by providing nutrition, creating a hostile environment for incoming bacterial pathogens, and modulating maturation of secondary lymphoid organs (Kim et al., 2017; Littman and Pamer, 2011). Importantly, microbiota is among the factors influencing development of tumors. The gut microbiota has been implicated in progression of cancers of the gut and associated organs. That effect is achieved by induction of inflammation through pattern-recognition receptors and metabolites that lead to induction of inflammatory cytokines and chemokines, or through production of DNA-damaging reactive oxygen and nitrogen species (Arthur et al., 2012; Hope et al., 2005; Rakoff-Nahoum and Medzhitov, 2007; Reddy et al., 1975; Yoshimoto et al., 2013). The gut microbiota can also be tumor suppressive (Donohoe et al., 2014) or enhance the effect of anti-cancer immunotherapy by modifying dendritic cell

maturation and promoting tumor-specific T cell responses (Sivan et al., 2015; Vetizou et al., 2015).

Some oncogenic retroviruses take advantage of the microbiota for their spread and replication. Previously, we demonstrated that transmission of mouse mammary tumor virus (MMTV), which causes mammary carcinomas in susceptible mice via insertional mutagenesis, depends on the gut commensal bacteria (Kane et al., 2011). Orally transmitted MMTV binds bacterial lipopolysaccharide (LPS) through LPS binding receptors incorporated into the viral membrane during budding (Wilks et al., 2015). LPS attached to the viral membrane triggers TLR4 to induce inhibitory cytokine interleukin-10 (IL-10), thus generating a status of immunological tolerance to the virus (Kane et al., 2011). Therefore, the microbiota enables successful virus replication and, thus, subsequent tumorigenesis by suppressing the anti-viral immune response.

In this study, we sought to determine whether the commensal microbiota influences replication and/or pathology induced by a retrovirus capable of transmitting through the blood–murine leukemia virus (MuLV) (Buffett et al., 1969; Duggan et al., 2006). Commensal microbiota was involved in control of MuLV in virus-resistant mice (Young et al., 2012), but the goal of our studies was to determine whether the microbiota influence the viral replication and pathogenesis in virus-susceptible mice. To elucidate the role of the microbiota on MuLV infection and associated pathology, Rauscher-like MuLV (RL-MuLV), which causes erythroid leukemia in mice from susceptible backgrounds (Hook et al., 2002) was used. Here, we established that while the gut microbiota had no effect on replication and transmission of the virus, it significantly enhanced virally induced leukemia development. The tumor progression was aided by select gut commensal bacteria, which upregulated signaling pathways counteracting the immune response capable of restricting leukemia development.

RESULTS

Microbiota is not required for MuLV transmission or replication

We have previously shown that the replication of a different retrovirus (MMTV) was dependent on the presence of the host microbiota, which served as a source of LPS used by MMTV to dampen the host’s immune response. If a similar scenario (control of replication by the microbiota) was applicable to MuLV, it would be difficult to study a potential role of the microbiota in development of MuLV-induced pathology. To address the issue, we used BALB/cJ mice either treated with microbiota-depleting doses of antibiotics (Abx) (Kane et al., 2011) or reared in germ-free (GF) conditions. SPF and GF mice were infected by intraperitoneal (i.p.) injection of 0.22 μm filter-sterilized MuLV as adults (G0 mice) and bred to produce offspring (G1 mice). SPF G1 mice, which were weaned either on regular or Abx-containing water, were examined for the presence of infectious virus along with GF G1 mice. This experimental design allowed us to test whether the microbiota is required for both virus replication and transmission. Frequency of infected cells and viremia were compared via infectious center and plaque assays, respectively (Rowe et al., 1970). Abx had no effect on viral replication in SPF mice compared with untreated SPF mice (Figure 1A). Furthermore, GF MuLV-infected mice also showed similar frequency of infected cells in

the spleens (Figure 1A) and infectious virions in the plasma (Figure S1A) compared with infected SPF mice. Thus, the system was robust for testing the role of the microbiota in leukemogenesis caused by MuLV.

Microbiota accelerates virally induced leukemia

Upon RL-MuLV infection, hematopoiesis within the bone marrow is blocked, resulting in compensatory extramedullary hematopoiesis (EMH) in the spleen (Hook et al., 2002). EMH leads to expansion of target cells susceptible to infection. RL-MuLV readily replicates within the rapidly proliferating erythroid progenitor cells, increasing the likelihood of proviral integration near a cellular proto-oncogene, a step necessary for development of erythroid leukemia as this virus does not encode an oncogene (Figure S1B).

To test whether the microbiota has an effect on RL-MuLV pathogenesis, mice from different groups were infected by i.p. injection of filter-sterilized virus as adults (G0 mice) and bred to produce infected offspring (G1 mice) that were further observed for leukemia development. G1 mice, which received a physiologically relevant infectious virus dose from their parents, were aged and monitored for leukemia. Diseased mice removed from the cohorts, and mice surviving up to 150 days were examined according to a leukemia scoring system, which was based on histological analysis of the spleen. Uninfected mice retained splenic architecture and were given a score of 0. Pre-leukemic mice were defined as having increased EMH and were given a score of 1. Leukemic mice exhibiting regions containing leukemic blasts with high mitotic activity were scored as 2, and more advanced cases, where the splenic architecture was wholly disrupted by immature leukemic blasts, were scored as 3 (Figure S1C). Leukemia score directly correlated with the spleen weight and all animals with a spleen weight greater than 0.35 g had leukemia (score 2/3) (Figures S1D–S1F).

Infected SPF BALB/cJ mice exposed to water containing a broad-spectrum Abx cocktail since weaning as well as infected GF BALB/cJ mice had increased latency of the disease and markedly reduced spleen weights compared with infected untreated SPF mice (Figures 1B, 1C, and S1G). As the leukemia-resistant phenotype of Abx-treated and GF mice was not due to a reduction in viral replication (Figures 1A and S1A), it became obvious that the microbiota significantly augmented viral pathogenesis.

Gut commensal bacteria differ in leukemia-promoting properties

The commensal microbiota is composed of various microorganisms, including bacteria, viruses, archaea, fungi, and unicellular eukaryotes. Antibiotics generally target bacterial microorganisms; however, metronidazole used in our Abx cocktail has also been shown to target protozoan species (Samuelson, 1999). To determine whether bacteria rather than protozoa promote MuLV-induced leukemia development in SPF mice, GF mice were colonized with a defined consortium of mouse commensal bacteria, altered Schaedler's flora (ASF) (Dewhirst et al., 1999), bred, and infected with filter-sterilized virus (G0 mice). Virus fate and pathogenesis was followed in G1 mice generated from infected G0 females. ASF restored susceptibility of GF mice to leukemia (Figures 1D and S1H), proving that commensal bacteria promote virally induced leukemogenesis. Potential differences in

kinetics of disease development in infected ASF versus SPF mice have not been analyzed beyond 100 days.

ASF contains seven bacterial species that include both Gram-positive and Gram-negative lineages (Sarma-Rupavtarm et al., 2004). A single Gram-positive bacterium, *Lactobacillus murinus*, and a single Gram-negative bacterium, *Parabacteroides goldsteinii*, were isolated from ASF and used to colonize GF mice. Progeny from *L. murinus*-colonized females developed leukemia at a similar rate and incidence as infected SPF mice (Figures 1E and 1F). Conversely, progeny from infected *P. goldsteinii*-colonized females exhibited leukemia development similar to that of infected GF mice (Figures 1E and 1F). Importantly, infected SPF and *P. goldsteinii*-colonized mice had similar frequency of infected splenocytes (Figure S1I). A non-member of ASF, the Gram-negative commensal *Bacteroides thetaiotaomicron* (*B. theta*) also conferred leukemia susceptibility to GF-infected mice (Figures 1E and 1F), although with a slight delay in disease development. These data provide evidence that leukemia-promoting factors are not inherent to all bacteria but are unique to certain bacteria across different bacterial phyla.

Erythroid differentiation is stalled at a specific stage of development in infected SPF mice

To study the promotion of leukemogenesis by commensal bacteria, we sought to determine the stage of erythroid leukemia development that is halted in infected GF mice. EMH is a result of MuLV-induced proliferation of hematopoietic stem cells (HSCs) in the spleen and occurs in 100% of RL-MuLV-infected BALB/cJ SPF mice (Hook et al., 2002). Both infected SPF and GF mice exhibited a robust expansion of HSCs, identified as the Sca-1^{+} population within nucleated spleen cells (Figure 2A), indicating that this phase in disease development was not affected in GF mice. In addition, BALB/cJ GF mice did not have a defect in the frequency of HSCs within the bone marrow (Figures 2B and S2A) or in differentiation of HSCs into hematopoietic lineages upon transfer into lethally irradiated mice (Figures 2C and S2B).

To further define the stage where disease development is blocked in GF mice, erythrocyte maturation in infected and uninfected SPF and GF mice was assessed by FACS analysis. During erythrocyte development, precursor cells initially express high levels of the transferrin receptor, CD71. As erythroid cells mature, they increase expression of an erythrocyte-specific marker (Ter119) and subsequently decrease CD71 expression (Zhang et al., 2003). Five distinct populations of cells in Figure 2D are defined by their characteristic staining patterns: $CD71^{med}TER119^{low}$ (gate R1), $CD71^{high}TER119^{low}$ (gate R2), $CD71^{high}TER119^{high}$ (gate R3), $CD71^{med}TER119^{high}$ (gate R4), and $CD71^{low}TER119^{high}$ (gate R5) during erythroid maturation (Zhang et al., 2003). Splenocytes from MuLV-infected SPF mice were stalled at stages R1 and R2 of the developmental process (Figures 2D, 2E, and S2C). Therefore, the majority of SPF-infected mice developed leukemias characterized as $CD71^{high}TER19^{low}$ and a small fraction developed $CD71^{high}TER19^{high}$ leukemias (Figure 2D). In contrast, significantly fewer infected GF mice have their spleen cells stalled at stages R1 and R2 (Figures 2D and 2E). This illustrates that the development of erythroid precursors is halted at the R1 stage of erythroid burst-forming units and erythroid colony-forming units and the R2 stage

corresponding to proerythroblasts and basophilic erythroblasts in the presence of the virus and microbiota.

Proinflammatory cytokine IL-6 is dispensable for leukemia development

Tumor promotion is often linked to chronic inflammation, which is defined as a prolonged, aberrant protective response to a loss of tissue homeostasis (Medzhitov, 2008). Inflammation-driven tumor promotion activates transcription factors in premalignant cells, which induce genes stimulating cell proliferation and survival (Grivennikov et al., 2010). One candidate factor that contributes to inflammation and tumorigenesis, is the proinflammatory cytokine IL-6. IL-6 has been shown to be overexpressed by host cells within the tumor microenvironment and by tumors of various etiologies (Lippitz, 2013), and also shown to be microbially induced and necessary for pre-leukemic myeloproliferation in genetically susceptible mice (Meisel et al., 2018). To determine the role of IL-6 in virally induced leukemia, IL-6-sufficient and -deficient female mice were infected with RL-MuLV and their progeny were monitored for leukemia. IL-6-sufficient and -deficient mice both developed leukemia at the same latency and with similar incidence (Figure 3A). Interestingly, while about 50% of infected SPF BALB/cJ wild-type (WT) mice develop leukemia by 150 days (Figure 1B), we noticed that nearly 80% of SPF BALB/c IL-$6^{-/-}$ mice exhibit leukemia by 150 days (Figure 3A). This could be attributed among other possibilities to the difference in strain background between BALB/cJ (the background strain used for all mice in the studies) and BALB/cByJ mice (the background strain of the IL-$6^{-/-}$ mice) that could influence the microbiota altering the rate of leukemia development. We also measured levels of IL-6 as well as other cytokines in the sera of uninfected, infected, and leukemic SPF BALB/cJ WT mice only to find that the cytokine concentration was unchanged (Figures 3B and S3). Therefore, in the case of RL-MuLV-driven leukemogenesis, the proinflammatory cytokine IL-6 can be ruled out as a contributing factor.

Commensal bacteria help tumors to escape the immune response

Maintenance of pre-cancerous and cancerous cells within the host requires the evasion or suppression of the immune response (Kim et al., 2007; Shankaran et al., 2001). To test the role of the adaptive immune response in resistance of GF mice to RL-MuLV-induced leukemia, we monitored leukemia development in immunodeficient RAG1 recombinase-negative (lacking a functional adaptive immune system) GF BALB/cJ G1 mice born to infected RAG1-deficient G0 mice. RAG1 deficiency led to enhanced susceptibility of RL-MuLV-infected GF mice to leukemia (Figures 3C and 3D). Importantly, both GF and SPF RAG$1^{-/-}$ mice displayed a similar frequency of infected splenocytes, excluding the possibility that the sensitivity of RAG1-deficient mice to MuLV-induced tumors could be simply explained by an increase in viral replication in these mice (Figure 3E).

These data implied that increased leukemia susceptibility in SPF mice was a consequence of commensal bacteria suppressing the anti-tumor adaptive immune response. And, conversely, the absence of commensal bacteria in GF mice allowed an unsuppressed adaptive immune response to counteract the development of leukemia. Even though MuLV induces immunosuppression in SPF mice (Dittmer et al., 2004; Robertson et al., 2006), the immune response still controls leukemia development to a certain degree as SPF RAG$1^{-/-}$

mice exhibited increased leukemia susceptibility compared with SPF RAG1-sufficient mice (Figures 3C and 3D). This response was unrelated to virus-specific antibodies (Abs) as neither infected GF nor SPF mice mounted virus-specific Ab responses (Figure 3F). In addition, significant susceptibility of GF RAG1$^{-/-}$ mice to RL-MuLV-induced leukemia ruled out the possibility that resistance of GF WT mice to leukemia is due to the lack of provirus integration in the vicinity of oncogenes.

MuLV infection and the microbiota produce a unique gene expression signature

To identify microbiota-mediated signaling pathway(s) essential for counteracting the immune response controlling leukemia progression, RNA-seq was performed on spleens from infected and uninfected age-matched GF and SPF mice (GF, GF MuLV, SPF, SPF MuLV) at the pre-leukemic stage (Figure 4A). Given the distinct phenotype of MuLV-infected SPF mice, we sought to identify gene expression changes associated with both microbiota and viral infection. A series of heuristic gene set filters were applied to the set of all genes across all mice. First, we assembled a set of genes that changed collectively between SPF MuLV mice and mice from the SPF, GF, and GF MuLV conditions (log-fold change > 0.5 and p 0.05 Wilcoxon rank sum test): intersection of (1) SPF MuLV versus SPF, (2) SPF MuLV versus GF, and (3) SPF MuLV versus GF MuLV (Figure 4A, positive gene set). Second, we assembled the group of genes from GF, GF MuLV, and SPF mice that differed from SPF MuLV condition (log-fold change > 0.5 and p 0.05 Wilcoxon rank sum test): union of (4) GF MuLV versus GF, (5) SPF versus GF MuLV, and (6) SPF versus GF (Figure 4A, negative gene set). Finally, we subtracted the negative gene set from the positive gene set, yielding candidate genes that were specifically influenced by the presence of both the virus and the microbiota. Knowing that leukemogenesis depends on the negative regulation of the immune response, we focused on genes that were known to have properties of negative immune regulation (Figure 4B, red arrows). Three genes–V-set immunoglobulin domain-containing 4 (VSig4), serine (or cysteine) peptidase inhibitor, clade B, member 9b (Serpinb9b), and RING finger protein 128 (Rnf128, also known as gene related to anergy in lymphocytes, or GRAIL) were selected for further *in vivo* analysis.

Deficiency in Serpinb9b or Rnf128 is sufficient to confer leukemia resistance in SPF mice

VSig4 was discovered as a complement receptor and subsequently shown to inhibit T cells (Vogt et al., 2006; Zeng et al., 2016). Serpinb9b is a serine protease inhibitor that acts on and suppresses granzyme M (Bots et al., 2005). Rnf128 is a ubiquitin ligase that, among many functions, has been shown to ubiquitinate CD3 and CD40L on T cells, leading to their degradation (Lineberry et al., 2008; Nurieva et al., 2010). To confirm the upregulation of these genes by MuLV and the microbiota, real-time quantitative PCR (qPCR) was performed using RNA isolated from the spleens of pre-leukemic mice. Whereas SPF pre-leukemic mice showed significant upregulation of these genes compared with uninfected SPF mice (Figure 4C, top), GF pre-leukemic mice did not (Figure 4C, bottom). Notably, the expression of VSig4, Serpinb9b, and Rnf128 was also upregulated in the spleens of *L. murinus*-colonized mice but not *P. goldsteinii*-colonized mice (Figure 4D) indicating that their induction correlated with the presence of bacteria with leukemia-promoting properties. Interestingly, Rnf128 was the only factor upregulated in the spleens of ex-GF mice colonized with leukemia-promoting *B. theta* (Figure 4D). Together, these data suggest

that one or a combination of these negative immune regulators function in a microbiota-dependent fashion to promote leukemia development.

To provide definitive proof that all or some of these genes (VSig4, Serpinb9b, and Rnf128) function to promote leukemia, a CRISPR-Cas9 approach was taken to generate BALB/cJ mice lacking these genes with the expectation that elimination of the critical factor(s) would result in leukemia resistance even in the presence of commensal bacteria. Guides were designed to target exon 1 of VSig4 (Figures S4A and S4D), exon 2 of Serpinb9b (Figure S4B), and the RING finger domain within exon 4 of Rnf128 (Figure S4C) resulting in frameshifting indels (VSig4 and Serpinb9b) and disruption of a functionally important domain of Rnf128 (Anandasabapathy et al., 2003). Mice with targeted mutations, their WT littermates, and BALB/cJ mice bred in the same colony were injected with the virus and further bred to produce infected offspring monitored for leukemia. VSig4-deficient mice developed leukemia at a similar latency and incidence as VSig4-sufficient mice (Figures 5A, 5B, and S4E), indicating VSig4 by itself does not contribute to MuLV-induced leukemia development. Interestingly, latency and incidence of leukemia development in Serpinb9b-deficient SPF mice and Rnf128-deficient SPF mice were both significantly delayed and reduced compared with WT mice (Figures 5A, 5B, and S4F). Rnf128 was specifically upregulated in $CD4^+$T cells (Figure 5C), supporting a role for Rnf128 in mediating $CD4^+$T cell unresponsiveness as previously reported (Kriegel et al., 2009; Nurieva et al., 2010). Serpinb9b was not upregulated in B cells, T cells, macrophages, or NK cells (Figure 5D). Furthermore, Serpinb9b upregulation was maintained in SPF $RAG1^{-/-}$-infected mice, ruling out a role for NKT cells (Figure 5E). Remaining cells in the spleen include monocytes such as neutrophils and dendritic cells. These cells constitute a small fraction of total splenocytes and are unlikely to be the source of Serpinb9b expression. Thus, Serpinb9b deficiency and Rnf128 deficiency significantly reduced leukemia susceptibility in SPF conditions without affecting viral replication (Figure S4G).

Serpinb9b is upregulated via the RIPK2 signaling pathway

To ascertain how the host detects microbially derived factors, which subsequently leads to upregulation of negative immune regulators, we investigated the role of host innate immune receptors in RL-MuLV-induced leukemia. Given that bacteria are sufficient to promote RL-MuLV-induced leukemia, we investigated pattern-recognition receptors that specifically detect bacterial moieties. We hypothesized that removal of the host sensor detecting leukemia-promoting bacteria would result in resistance to leukemia even in the presence of the microbiota. Mice lacking innate immune receptors TLR2 and TLR4, and mice unable to signal through NOD1/2 via deficiency in the adaptor RIPK2, were bred on the BALB/cJ background, infected with RLMuLV, and their offspring were monitored for leukemia. Mice deficient in TLR2, a receptor for bacterial products including lipoteichoic acid and capsular polysaccharide (de Oliviera Nascimento et al., 2012; Graveline et al., 2007; Han et al., 2003), displayed latency and incidence of leukemia similar to WT SPF mice (Figures 6A and 6B). Similarly, TLR4-deficient mice, which are unable to detect LPS (Poltorak et al., 1998), exhibited leukemia latency and incidence similar to WT SPF mice (Figures 6A and 6B). However, it was possible that signaling through either TLR2 or TLR4 could be redundant and promote leukemia development. To address this possibility, we

infected TLR2$^{-/-}$ TLR4$^{-/-}$ mice and monitored their offspring for leukemia to find that they were as susceptible as mice deficient in either single receptor (Figures 6A and 6B).

At the same time, mice deficient in RIPK2, the downstream adaptor of intracellular peptidoglycan receptors NOD1 and NOD2 (Caruso et al., 2014), had significantly increased latency and decreased total leukemia incidence compared with WT SPF mice (Figures 6A and 6B). These data suggested that detection of microbial products, likely intracellular peptidoglycan, and signaling through the NOD1/2 RIPK2 pathway promoted RL-MuLV-induced leukemia development. Although RIPK2-deficient mice were significantly more resistant to leukemia development compared with WT SPF mice, RIPK2 deficiency did not confer the level of leukemia resistance observed in WT GF mice (Figures 6A and 6B). These data suggest that other innate immune sensors also play a role in RL-MuLV-induced leukemia development.

Next, we tested which of the negative immune regulators upregulated in MuLV-infected SPF mice were dependent on the RIPK2 signaling. Accordingly, RNA expression of the negative immune regulators in infected and uninfected RIPK2-deficient mice was compared. Whereas expression of Rnf128 and VSig4 was significantly upregulated in infected RIPK2-deficient mice (Figures S5A and S5B), expression of Serpinb9b was not (Figure 6C). Importantly, Serpinb9b was upregulated in infected RIPK2-sufficient control mice (Figure 6C). Together, these data demonstrate that activation of RIPK2 contributes to the upregulation of Serpinb9b in the presence of both the virus and commensal bacteria. Therefore, a lack of Serpinb9b upregulation in RIPK2-deficient mice is likely the basis for the observed increase in leukemia resistance.

DISCUSSION

Retroviruses induce a broad range of tumors in vertebrates. In most cases, retroviruses induce tumors by insertional activation of cellular proto-oncogenes during establishment of a provirus. Importantly, these proto-oncogenes are implicated in spontaneous tumors in humans. Although proto-oncogene upregulation constitutes a necessary step for initiation of retrovirally induced tumorigenesis, additional events–tumor promotion and progression (Kinzler and Vogelstein, 1996)–are required for successful tumor formation. Tumor promoters enhance cell survival and may induce clonal expansion of precancerous cells, whereas tumor progression is caused by additional mutations, which enable cancerous cells to invade neighboring tissues and metastasize.

The ability of the microbiota to regulate viral replication and pathogenesis caused by viruses belonging to different families (Baldridge et al., 2015; Kane et al., 2011; Kuss et al., 2011; Uchiyama et al., 2014) initiated our interest in its influence on MuLV-driven pathology. Some older literature suggested that the microbiota could influence MuLV-induced leukemia development, but it was highly controversial: GF animals infected with Friend's MuLV (F-MuLV) either exhibited greater disease severity (Mirand and Grace, 1963) or milder disease (Isaak et al., 1988; Kouttab and Jutila, 1972) than their SPF control mice. Several factors may explain the discordance: at that time viral stocks were likely contaminated with lactate dehydrogenase-elevating virus (Dittmer et al., 2019), which is known to suppress and

delay $CD8^+$T cell responses against F-MuLV, prolonging acute viral infection (Robertson et al., 2008). Furthermore, in that pre-PCR and sequencing era the sterility of the experimental isolators was tested only using culturing techniques (Kouttab and Jutila, 1972). Thus, unculturable bacteria could have been missed.

In our studies of retrovirally induced leukemia that originates in an organ distant from the gut, we found that the intestinal commensal bacteria enhanced the leukemogenesis. In contrast to experiments in which the microbiome supported viral replication (Baldridge et al., 2015; Kane et al., 2011; Kuss et al., 2011; Uchiyama et al., 2014), we found that the decreased leukemogenesis observed in RL-MuLV infected GF mice could not be explained by a decrease in the virus burden. Instead, we discovered that the microbiota promotes leukemia development by negatively controlling the immune response. The immune system plays a role in controlling tumors of various etiology at each of the steps of tumor development (Vinay et al., 2015). Under its pressure, tumor cells exploit multiple mechanisms of avoidance of the immune responses: induction of regulatory T cells (Jacobs et al., 2012), defective antigen presentation due to down-modulation of antigen processing machinery (Hicklin et al., 1999; Johnsen et al., 1999), production of immunosuppressive mediators (Lind et al., 2004; Pasche, 2001), to name a few.

The high susceptibility and rapidity with which RL-MuLV-infected GF $RAG1^{-/-}$ mice develop leukemia supports a role for cells expressing somatically rearranged immune receptors in controlling tumor development in GF mice: T cells, B cells, and cells carrying rearranged receptors but resembling innate cells, such as NKT cells. As neither SPF nor GF infected virus-susceptible mice produce neutralizing antibodies against viral antigens (Figure 3F), any prominent role for B cells in protective anti-tumor immune response seems unlikely. The absence of virus-neutralizing antibodies also explains the lack of control of extracellular virions in GF and SPF mice enabling the virus to spread from cell to cell. Therefore, the adaptive immune response against MuLV pathogenesis is likely controlled by T cells and/or NKT cells. Anti-tumor immune responses by NKT cells are thought to be primarily through their support of other effector cells like $CD8^+$ T cells and NK cells via production of Th1 cytokine IFN-γ (Crowe et al., 2002) or IL-2 (Metelitsa et al., 2001). Both $CD4^+$ T cells and $CD8^+$ T cells play decisive roles in suppressing tumor development and growth (Toes et al., 1999). $CD4^+$T cells contribute to anti-tumor immunity by secretion of proinflammatory cytokines such as IL-2, IFN-γ, and TNF-α (Quezada et al., 2010). $CD4^+$ T cells have also been reported to adopt cytotoxic activity by means of Fas-mediated cell death or perforin and granzymes induced apoptosis (Nagata and Golstein, 1995; Raskov et al., 2021; Xie et al., 2010). That said, RAG deficiency has been associated with reduced functionality of NK cells (Karo et al., 2014), suggesting that this cytotoxic cellular subset could also be targeted by microbiota-driven tumor-promoting negative immunoregulation.

RNA-seq analysis revealed three negative immune regulators (VSig4, Rnf128, and Serpinb9b) the expression of which was significantly increased in the presence of both the virus and the microbiota. Rnf128 and Serpinb9b proved to be critical for leukemia development in RL-MuLV-infected SPF mice (Figure 5A). In line with our results, overexpression of the members of the ovalbumin family of serpins, to which Serpinb9b belongs, as well as Rnf128, are markers for poor prognosis in some human cancers

([Bai et al., 2020; ten Berge et al., 2002; Uhlen et al., 2017] and our own analysis of previously published data [Bolouri et al., 2018]). A homolog for Serpinb9b has not been identified in humans, but related family member, human proteinase inhibitor 9 (SerpinB9) inhibits perforin-mediated cytotoxic T lymphocyte cytotoxicity (Medema et al., 2001). In addition, murine Serpinb9 was shown to protect mouse melanoma tumors from granzyme B-mediated killing (Jiang et al., 2020). Published data support the idea that Serpinb9b functions in a similar manner by inhibiting the action of granzymes toward tumors (Bots et al., 2005). Rnf128 is highly expressed in anergic T cells and ubiquitinates key activation signaling molecules, such as CD3, resulting in their degradation (Nurieva et al., 2010). Rnf128-deficient primary $CD4^+$ T cells do not develop anergic phenotype in various models and also exhibit hyperactivation upon TCR stimulation (Kriegel et al., 2009). Rnf128 deficiency in $CD8^+$ T cells enhances their anti-tumor effector function by increasing expression of IFN-γ, granzyme B, perforin 1, and TNF-α (Haymaker et al., 2017). Precisely how Serpinb9b and Rnf128 function in the context of MuLV infection is yet to be discovered. We hypothesize that Serpinb9b upregulation in tumor progenitor cells prevents killing by cytotoxic granzymes and Rnf128 upregulation in $CD4^+$ T cells likely induces unresponsiveness is these T cells, suppressing the immune response and enabling leukemia development (Figure 7). Defining the stage at which commensal bacteria initiate immunosuppression is a subject of future studies.

Although VSig4 is a bona fide negative regulator (Vogt et al., 2006), $VSig4^{-/-}$ mice were as susceptible as WT littermates to RL-MuLV-induced leukemia (Figure 5A). It is possible that VSig4 serves as a marker of cells that have immunosuppressive function that is independent of VSig4. For example, $VSig4^+$ resident macrophages have documented immunosuppressive function in various experimental models (Chen et al., 2010, 2011; Fu et al., 2012; Vogt et al., 2006; Xu et al., 2010).

Since bacterial products stimulate multiple innate pattern-recognition receptors, it is important to understand which particular pathway(s) is necessary for promotion of leukemogenesis. Our studies illustrated a role for RIPK2, but not TLR2 or TLR4, in promoting MuLV-induced leukemia development. In contrast to our studies, two prior reports, which examined the effect of the NOD/RIPK2 pathway on tumors in the colon and liver, demonstrated a suppressive effect of this signaling on tumor development (Chen et al., 2008; Ma et al., 2015). The mechanism by which activation of this pathway influenced tumor development was distinct in the two models of tumorigenesis. Erythroblastic leukemia originates from erythroid precursors found in infected spleens and the bone marrow (Hook et al., 2002), locations distant from the gut potentially explaining the discrepancies. RIPK2 likely supported leukemia development through upregulation of the negative immune regulator Serpinb9b as its expression was increased in WT but not RIPK2-deficient MuLV-infected SPF splenocytes. The RIPK2-Serpinb9b signaling axis does not entirely explain the high susceptibility of SPF mice to leukemia compared with GF mice: the development of leukemia in RIPK2-deficient SPF mice was significantly reduced but did not reach the low level of GF animals (Figure 6B). Thus, additional signaling pathways must contribute to bacteria-dependent promotion of leukemogenesis. This pathway most likely involves Rnf128, which was the only negative regulator upregulated in infected *B. theta*-colonized gnotobiotic mice susceptible to leukemia (Figure 4D).

Importantly, the bacterial factors promoting leukemia development are not intrinsic to Gram-positive or Gram-negative bacteria, as members from both groups confer leukemia susceptibility. Furthermore, bacteria belonging to the same order of Bacteroidales, *P. goldsteinii* and *B. theta*, exhibit different leukemia-promoting capabilities. A major difference between the two Bacteroidales bacteria utilized in this study is the presence of an S-layer in *P. goldsteinii* (Fletcher et al., 2007). The S-layer is a bacterial cell structure composed of protein or glycoprotein thought to have evolved to provide protection against environmental factors (Fletcher et al., 2007; Sleytr et al., 1993) and the host's immune response (Ezeji et al., 2021). Thus, the S-layer may prevent proinflammatory signaling (Cuffaro et al., 2020; Kverka et al., 2011) and upregulation of the negative regulators in response to it. In addition, peptidoglycan composition and levels of peptidoglycan released from the bacteria differ greatly between bacteria and, thus, may influence their NOD1/2 stimulatory capability (Hasegawa et al., 2006; Lee et al., 2009). Furthermore, some bacteria are able to directly secrete NOD1/2 ligands into host cells (Caruso et al., 2014). It seems obvious that commensals capable of downregulation of adaptive immune responses by upregulating the described negative regulators do so to maintain tolerance to themselves. Tumor promotion is obviously a side effect that requires additional genomic events stimulated by the retroviral infection.

In summary, our study highlights a role for the microbiota in the pathogenesis of a retrovirus in the absence of decreased virus replication. In this study, for the first time, we demonstrate that commensal bacteria facilitate leukemia development via induction of negative regulators of the immune response–a novel gut microbiota-mediated mechanism that enables tumor progression. As these negative regulators can be linked to a poor prognosis in certain human cancers (Bai et al., 2020; ten Berge et al., 2002; Uhlen et al., 2017), it is likely that similar mechanisms of immune evasion operates in tumors induced by viruses and potentially in spontaneous tumors of non-viral origin.

Limitations of the study

Despite our rigorous findings, this study has a few limitations. By using mice colonized with a defined and well-characterized consortium like ASF, we were able to further investigate the mechanism by which certain bacteria confer MuLV-induced leukemia development. However, our reductionist approach limited us from generating a bacterial consortium originating from our SPF animal facility. Therefore, bacterial species (besides *L. murinus* present in all mouse colonies throughout the globe) driving leukemia development in SPF mice remain to be determined.

STAR★METHODS

RESOURCE AVAILABILITY

Lead contact—Additional information and requests for resources and reagents should be directed and will be fulfilled by the lead contact, Tatyana Golovkina (tgolovki@bsd.uchicago.edu).

Materials availability—All unique/stable reagents generated in this study are available from the lead contact with a completed materials transfer agreement.

Data and code availability—Splenic RNA-seq datasets from SPF infected, GF infected, SPF uninfected, and GF uninfected mice have been deposited at NCBI Gene Expression Omnibus (GEO) database, accession ID GSE209752. This paper does not report original code. Any additional information required to reanalyze the data reported in this paper is available from the lead contact upon request.

EXPERIMENTAL MODEL AND SUBJECT DETAILS

Mice utilized in this study were bred and maintained at the animal facility of The University of Chicago. BALB/cJ mice were purchased from The Jackson Laboratory (TJL). C.129S7(B6)-*Rag1*^{tm1Mom}/J, C.C3-*Tlr4*$^{Lps\text{-}d}$/J, C.129(B6)-*Tlr2*^{tm1Kir}/J, and B6.129S1-*Ripk2*^{tm1Flv}/J mice were purchased from TJL and backcrossed to BALB/cJ mice for 10 generations to create RAG1$^{-/-}$, TLR4$^{-/-}$, TLR2$^{-/-}$, and RIPK2$^{-/-}$ mice, respectively, on the BALB/cJ background. TLR2$^{-/-}$ and TLR4$^{-/-}$ mice on the BALB/cJ background were intercrossed to produce double deficient mice. CByJ.129S2(B6)-IL6^{tm1Kopf}/J, purchased from TJL were crossed to BALB/cJ mice and the resulting F1 mice were intercrossed to generated −/− and +/+ littermate mice used in the studies.

Serpinb9b$^{-/-}$, Rnf128$^{-/-}$, and VSig4$^{-/-}$ BALB/cJ mice were generated using the CRISPR/Cas9 approach. To generate VSig4$^{-/-}$ mice, two guide RNAs targeting exon 1 (5′AGAAGTAGCTTCAAATAGGA-3′ and 5’TGAGCACTATTAGGTGGCCC-3′) were used (Figure S4A). Five distinct BALB/cJ VSig4$^{-/-}$ lines were produced. Primers flanking exon 1 (5′CCAGAACAAATGGTTTCCCTAG-3′ and 5′TTGGAGTCCTCTGACATCCC-3′) were used to genotype the founder mice and subsequent offspring. Equal numbers of mice from each line were used in all experiments.

To generate Serpinb9b$^{-/-}$ mice, two guide RNAs were used to target exon 2 (5′TATGGTCCTCCTGGGTGCAA-3′ and 5′TTCCACCCTAGTTGTTACTC-3′) (Figure S4B). Genotyping was performed using two primers flanking exon 2 (5′TTTCCCTCCAGACTCTGCA-3′ and 5′GAGAAGCATGAGGCCAAGAC-3′). Two lines of Serpinb9b$^{-/-}$ mice were produced. Equal numbers of mice from both lines were used in all experiments.

For the generation of BALB/cJ Rnf128$^{-/-}$ mice, one guide RNA was used to target exon 4 (5′AGGATGCGCACCAAATCATT-3′)(Figure S4C). Founder mice and their offspring were genotyped using primers flanking exon 4 (5′AGTCACACCTCACTCTTTATCCA-3’ and 5′TCGAGAACAAACTGTACCGGA-3′). One line of Rnf128$^{-/-}$ mice was developed. Founder VSig4$^{-/-}$, Serpinb9b$^{-/-}$, and Rnf128$^{-/-}$ mice were crossed to BALB/cJ mice for at least two generations. Heterozygous mice were then intercrossed to produce homozygous knockout (KO) animals used in subsequent studies.

Males and females were used at ~50:50 ratio in all experiments. The age of mice used in each experiment ranged from 3–5 months. Specific ages are indicated in the respective

figure legend. The studies outlined here have been reviewed and approved by the Animal Care and Use Committee at The University of Chicago.

METHOD DETAILS

Antibiotic treatment—BALB/cJ females injected intraperitoneally (i.p.) with 1×10^3 plaque forming units (pfus) of RL-MuLV were bred with BALB/cJ males to produce infected G1 animals. The G1 mice were weaned onto water containing the following antibiotic mixture: kanamycin (4 mg/mL), gentamicin (3.5 mg/mL), colistin (8500 U/mL), metronidazole (2.15 mg/mL), and vancomycin (4.5 mg/mL) for the duration of the experiment. When the mice became symptomatic (anemic, lethargic, enlarged abdomen), they were sacrificed and assessed for leukemia development. All animals were sacrificed by 5 months of age. The efficacy of the antibiotic-treatment protocol was evaluated by periodical bacteriologic examination of feces. Fresh fecal samples from antibiotic-treated and control mice were vortexed in TSA broth (0.1 g in 1 mL) and plated on BBL plates. Plates were incubated for 48 h at 37°C under both aerobic and anaerobic conditions. Anaerobic growth conditions were created using a COY anaerobic chamber (Grass Lake, MI). There were no detectable colony forming units (CFUs) on either aerobic or anaerobic plates from the antibiotic treated animals. The plates from the untreated animals had 10^7 CFUs and 8×10^5 CFUs of anerobic and aerotolerant bacteria per 1 g of feces, respectively.

Monitoring sterility in GF isolators—BALB/cJ and BALB/cJ RAG1$^{-/-}$ mice were re-derived as germ-free (GF) at Taconic and housed in sterile isolators at the gnotobiotic facility at the University of Chicago. Sterility of GF isolators was assessed as previously described (Wilks et al., 2014). Briefly, fecal pellets were collected from isolators weekly and quickly frozen. DNA was extracted using a bead-beating/phenol-chloroform extraction protocol. A set of primers that broadly hybridize to bacterial 16 S rRNA gene sequences were used to amplify isolated DNA. In addition, microbiological cultures were set up with GF fecal pellets, positive control SPF fecal pellets, sterile saline (sham), and sterile culture medium (negative control). BHI, Nutrient, and Sabbaroud Broth tubes were inoculated with samples and incubated at 37°C and 42°C aerobically and anaerobically. Cultures were followed for five days until cultures were deemed negative.

Colonization of GF mice—GF BALB/cJ mice were colonized with the ASF consortium (Sarma-Rupavtarm et al., 2004) via oral gavage of suspended cecal contents from donor mice. All but one species (ASF360, *Lactobacillus acidophilus*) were found in the ASF-colonized mice. *Lactobacillus murinus* (*L. murinus*, ASF361) and *Parabacteroides goldsteinii* (*P. goldsteinii*, ASF519) were isolated from the ASF consortium. *L. murinus* was isolated by plating suspended fecal matter from ASF-colonized mice onto de Man, Rogosa and Sharpe agar (MRS) (Thermo Fisher Scientific), a selective media for *Lactobacilli*. Growth of *L. murinus* was confirmed by PCR. *P. goldsteinii* was isolated by plating fecal matter from ASF colonized mice re-suspended in PBS onto brain heart infusion supplemented (BHIS) media, supplemented with hemin and vitamin K1, and grown in an anaerobic chamber. Growth of *P. goldsteinii* was confirmed by PCR. *Bacteroides thetaiotaomicron* (*B. theta*, VPI-5482 Δtdk) (Jacobson et al., 2018) was grown on tryptone yeast extract glucose (TYG) media in an anaerobic container. *L. murinus, P. goldsteinii*,

and *B. theta* were introduced to GF BALB/cJ mice by oral gavage of 200 μL of overnight liquid culture grown from single colonies. Successful colonization was confirmed via PCR using primers specific for each individual bacterium. Female offspring of colonized mice were infected with filter-sterilized virus (G0 mice), bred to produce G1 mice which were monitored for leukemia.

Virus isolation, infection, and leukemia monitoring—Rauscher-like Murine Leukemia Virus (RL-MuLV) which consists of N, B tropic ecotropic and mink cell focus forming (MCF) virus causing erythroleukemia in susceptible BALB/c mice (Hook et al., 2002; Ter-Grigorov et al., 1997) was isolated from tissue culture supernatant of infected SC-1 cells (ATCC CRL-1404). The virus was tested for hepatitis virus, mouse thymic virus, mouse parvovirus, pneumonia virus of the mouse, polyomavirus, mammalian orthoreovirus serotype 3, enzootic diarrhea virus of infant mice, Sendai virus, Mycoplasma (M) pulmonis, *M. arginine, M. arthritidis, M. bovis, M. cloacale, M. falconis, M. faucium, M. fermentans, M. genitalium, M. hominis, M. hyorhinis, M. hyosynoviae, M. opalescens, M. orale, M. pirum, M. pneumonia, M. salivarium, M. synoviae, Acholeplasma laidlawii, Ureaplasma urealyticum*, cilium-associated respiratory bacillus, ectromelia virus, encephalitozoon cuniculi, Theiler's murine encephalomyelitis virus, Hanta virus (Korean hemorrhagic virus), lymphocytic choriomeningitis virus, lactate dehydrogenase enzyme, minute virus of the mouse, mouse adenovirus, and mouse cytomegalovirus and was found to be negative for all the pathogens.

Ecotropic virus titers in the RL-MuLV mixture were determined by an XC infectious plaque assay as described in (Rowe et al., 1970). 1×10^3 pfus of the virus isolated from supernatants of infected SC-1 cells were injected i.p. into 6–8 week-old BALB/cJ mice (G0 mice). Mice were bred to produce G1 animals which were used as a source of the virus for all experiments. The virus was not passaged beyond G1 *in vivo*. To isolate the virus, splenic homogenates of non-leukemic 2-3-month-old G1 mice were centrifuged at 2,000 rpm for 15 min at 4°C. The supernatant was layered onto a 30% sucrose cushion and spun down at 31,000 rpm using a TW55.1 bucket rotor for 1 h at 4°C. The pelleted fraction was resuspended in PBS, which was spun at 10,000 rpm at 4°C to remove insoluble material. The resulting supernatant was aliquoted, titered and stored at −80°C.

Splenic derived RL-MuLV was diluted in sterile PBS and filtered through a sterile 0.22 μm membrane in a laminar flow hood. 1×10^3 pfus were injected i.p. into GF and SPF BALB/cJ females, which were used as controls in all experiments with gnotobiotic mice. For genetically altered mice, −/−, +/+, and in some instance +/− female littermates were injected i.p. with 1×10^3 pfus. In addition, non-littermate wild-type (WT) BALB/cJ mice bred in the colony were also infected and served as non-littermate controls. Infected females were put in mating to generate G1 animals. G1 +/+ and +/− littermates of G1 −/− mice were cohoused with −/− mice to normalize the microbiota through the course of the studies. G1 mice were aged and monitored for leukemia development which included signs of lethargy, hunched back, ruffled/unkempt fur, distended abdomen, and anemia. Symptomatic mice were sacrificed. All mice were sacrificed by 5months, at the conclusion of the experiment. Survival curves indicate symptomatic mice that were closed during 150days. The survival curve for SPF mice is a cumulative curve generated over the course of the entire study

using BALB/cJ mice. +/− and +/+ littermates were used for each of the experimental groups of genetically modified mice and their survival curves were compared with the cumulative curve for SPF mice to ensure that the leukemia development rate is the same (Figures S3E and S3F). Comparison between leukemia score and spleen weight indicate that spleen weights ≥ 0.35 g have a leukemia score of 2 or higher (Figures S1D–S1F), which was used for some wild-type BALB/cJ SPF and GF mice as a proxy for denoting leukemia. Leukemia or lack of it for all gnotobiotic, genetically modified and control SPF mice was also confirmed histologically using splenic sections.

Histology—Mouse spleens were fixed in Telly's fixative, sectioned, and stained with hematoxylin and eosin. Leukemia was scored using the following criteria: maintenance of splenic architecture, level of cellular mitotic activity and degree of cell maturation (Figure S1C).

Plaque and infectious center assays—Blood from RL-MuLV infected BALB/cJ mice was collected in tubes containing heparin, which was then spun at 10,000 rpm for 10 min at 4°C. The plasma was serially diluted in PBS, and was subjected to the XC plaque assay (Rowe et al., 1970).

To assess the frequency of infected cells, single cell suspensions (with red blood cells) from RL-MuLV infected mouse spleens were serially diluted in Clicks medium (Irvine scientific) and were subjected to the infectious center assay (Rowe et al., 1970).

Fluorescence-activated cell soring (FACS) analysis—For analysis of cells expressing hematopoietic stem cell (HSC) marker (Sca-1), single cell suspensions from mouse spleens were stained with fluorescein isothiocyanate (FITC)-conjugated anti-Ly-6A/E (Sca-1) mAb (Biolegend; San Diego, CA). To analyze erythrocyte maturation, splenocyte suspensions were stained with FITC-conjugated anti-CD71 (transferrin receptor) mAb (Biolegend; San Diego, CA) and phycoerythrin (PE)-conjugated anti-Ter119 (erythroid cells). Stages of erythrocyte maturation were determined as described in (Zhang et al., 2003). Regions R1 to R5 were defined by the following pattern: $CD71^{med}TER119^{low}$, $CD71^{high}TER119^{low}$, $CD71^{high}TER119^{high}$, $CD71^{med}TER119^{high}$, and $CD71^{low}TER119^{high}$, respectively. Dead cells (propidium iodide-positive) were excluded from the analysis. For analysis of VSig4 deletion in VSig4-deficient mice, peritoneal macrophages were stained with FITC-conjugated anti-F4/80 mab (Biolegend; San Diego, CA) and allophycocyanin (APC)-conjugated anti-VSig4 mAb (eBioscience; San Diego, CA).

Hematopoietic stem cells (HSC) quantification in GF and SPF mice—Bone marrow was isolated from SPF and GF mice. The red blood cells were lysed, and 2×10^7 cells were stained with the following monoclonal antibody (mAb) cocktail: peridinin-chlorophyll protein Cy5 (PerCP-Cy5) conjugated lineage specific mAbs (eBioscience; San Diego, CA) (CD11 c, NK1.1, CD11b, Ter119, CD3e, CD8a, CD19, TCRβ, TCRβ, B220, and Gr1), APC conjugated anti-Kit mAb (eBioscience; San Diego, CA), Phycoerythrin/Cy7 (PE/Cy7) conjugated anti-Sca-1 mAb (eBioscience; San Diego, CA), PE conjugated anti-Flt3 mAb (eBioscience; San Diego, CA). Dead cells (propidium iodide–positive) were

excluded from the analysis. HSCs were defined as lineage negative, Sca-1 and Kit positive, Flt3 negative cell population.

Identification of hematopoietic lineages in bone marrow chimeras—Single-cell suspensions were prepared from bone marrow from age- and gender-matched GF and SPF mice. Recipient SPF BALB/cJ mice irradiated at 900 rad received 2×10^6 BM cells intravenously. Nine days after the transfer, the mice were sacrificed. Their spleens and bone marrow were fixed in Bouin's fixative, sectioned, and stained with hematoxylin and eosin.

Staining of paraffin sections—Five-micron paraffin spleen sections were stained with a-GATA1 Ab, clone D52H6 (Cell Signaling) and counterstained with hematoxylin. Antigen was retrieved at low pH.

RNA sequencing—RNAseq analysis was performed on splenic RNA from infected (preleukemic, sore 1) and uninfected GF and SPF BALB/cJ males and females (4 groups of mice, 6–8 mice per group). Splenic RNA was subjected to Illumina Next Gen Sequencing to generate a Directional Total RNA library. Ribosomal RNA was removed using a Ribo-Zero rRNA removal kit (Epicentre; Madison, WI). Gene expression was quantified through the Kallisto software (Bray et al., 2016). To identify genes regulated by both the microbiota and the virus, we performed a series of heuristic gene set filtering operations (see explanation in the text) using log-fold change >0.5 and $p < 0.05$ Wilcoxon rank sum test. Gene filtering and statistical analysis was conducted using MATLAB (R2019b) (Natick, MA).

Measurement of serum cytokines—Serum cytokine levels were assessed in uninfected, pre-leukemic, and leukemic mice using a Cytometric Bead Array for mouse Th1, Th2, and Th17 cytokines (BD Biosciences; San Jose, CA) as per manufacturer's instructions.

Cell sorting—Cells were sorted using FACS or magnetic-activated cell sorting (MACS). For FACS sorted cells, red blood cell lysed splenocytes were stained with the following antibody cocktail: APF-Cy7 labeled anti-B220 (Biolegend; San Diego, CA), APC labeled anti-CD3 (Life Technologies Corp; Carlsbad, CA), and BV421 labeled anti-F4/80 (Biolegend; San Diego, CA). For MACS sorted cells, red blood cell lysed splenocytes were labeled using CD4 and CD8 antibody conjugated microbeads (Miltenyi Biotec; Bergisch Gladbach, Germany) and positively sorted as detailed by the manufacturer. NK cells were negatively sorted per manufacturer's instructions using an NK cell isolation kit (Miltenyi Biotec; Bergisch Gladbach, Germany). RNA from sorted cells was isolated and gene expression analyzed as described below.

RNA isolation from spleens and quantitative reverse transcription PCR (RT-qPCR)—RNA was isolated from spleens using either guanidine thiocyanate extraction and CsCl gradient centrifugation (Chirgwin et al., 1979) or Purelink RNA Mini Kit (Invitrogen). Complementary DNA (cDNA) was generated using SuperScript IV Reverse Transcriptase (Life Technologies). Real-time PCR was conducted either with TaqMan Master Mix (ThermoFisher) or SYBR green master mix (Bio-Rad; Hercules, CA). TaqMan primer pairs and probes to amplify VSig4

(Mm00625349_m1), Serpinb9b (Mm00488405_m1), Rnf128 (Mm00480990_m1), and Beta-Actin (Mm02619580_g1) were from Applied Biosystems. The following forward and reverse primers were used to amplify VSig4 - 5′-GGAGATCTCATCAGGCTTGC-3′ and 5′CCAGGTCCCTGTCACACTCT; Rnf128 - 5′TAGCTGTGCTGTGTGCATTG-3′ and 5′GAATGTCACACTTGCACATGG-3′; Serpinb9b - 5′AGCAGACCGCAGTCCAGATA-3′ and 5′GTCTGGCTTGTTCAGCTTCC-3′, and beta-actin - 5′GTATCCTGACCCTGAAGTACC-3′ and 5′TGAAGGTCTCAAACATGATCTG-3′ in SYBR green master mix reactions. cDNA was quantified using the comparative Ct method.

ELISA

An enzyme-linked immunosorbent assay (ELISA) was used to detect anti-MuLV antibodies in MuLV-infected GF and SPF BALB/cJ mice as previously described (Case et al., 2008). Briefly, RL-MuLV virions isolated from infected SC-1 cells were treated with 0.1% Triton X-100 and bound to plastic in borate-buffered saline overnight. Two percent ovalbumin was used as blocking component. Sera samples were incubated at 4°C for one hour at a 1×10^{-2} dilution, followed by goat anti-mouse IgGs coupled to horseradish peroxidase (HRP) (SouthernBiotech, Birmingham, AL). Background optical density (OD_{450}) values from incubation with secondary antibody alone were subtracted from values acquired from sera of infected mice.

QUANTIFICATION AND STATISTICAL ANALYSIS

Statistical tests were calculated using GraphPad software. Statistical details of experiments including statistical tests used, the value of n, what n represents, and the definition of center and dispersion measures are indicated in relevant figure legends.

Supplementary Material

Refer to Web version on PubMed Central for supplementary material.

ACKNOWLEDGMENTS

We thank members of the Golovkina and Chervonsky labs for helpful discussions, Emmily Shanks for technical help, Joseph Pickard and Helen Beilinson for editing the manuscript, and Barbara Kee and Renee de Pooter for help with HSC staining. We also thank GRAF at University of Chicago, which enable gnotobiotic studies. This work was supported by NIH grants R21AI138224 to T.G. and R01CA232882 to T.G. and M.F. J.S. and J.W. were supported by T32 GM007183 and T32 AI007090, respectively. This work was also supported by NIH/NIDDK Digestive Disease Research Core Center grant DK42086 and NIH grant P30CA014599.

REFERENCES

Anandasabapathy N, Ford GS, Bloom D, Holness C, Paragas V, Seroogy C, Skrenta H, Hollenhorst M, Fathman CG, and Soares L (2003). GRAIL: an E3 ubiquitin ligase that inhibits cytokine gene transcription is expressed in anergic CD4+ T cells. Immunity 18, 535–547. [PubMed: 12705856]

Arthur JC, Perez-Chanona E, Mühlbauer M, Tomkovich S, Uronis JM, Fan TJ, Campbell BJ, Abujamel T, Dogan B, Rogers AB, et al. (2012). Intestinal inflammation targets cancer-inducing activity of the microbiota. Science 338, 120–123. 10.1126/science.1224820. [PubMed: 22903521]

Bai X-S, Zhang C, Peng R, Jiang G-Q, Jin S-J, Wang Q, Ke A-W, and Bai D-S (2020). RNF128 promotes malignant behaviors via EGFR/MEK/ERK pathway in hepatocellular carcinoma. OncoTargets Ther. 13, 10129–10141. 10.2147/OTT.S269606.

Baldridge MT, Nice TJ, McCune BT, Yokoyama CC, Kambal A, Wheadon M, Diamond MS, Ivanova Y, Artyomov M, and Virgin HW (2015). Commensal microbes and interferon-lambda determine persistence of enteric murine norovirus infection. Science 347, 266–269. 10.1126/science.1258025. [PubMed: 25431490]

Bolouri H, Farrar JE, Triche T Jr., Ries RE, Lim EL, Alonzo TA, Ma Y, Moore R, Mungall AJ, Marra MA, et al. (2018). The molecular landscape of pediatric acute myeloid leukemia reveals recurrent structural alterations and age-specific mutational interactions. Nat. Med 24, 103–112. 10.1038/nm.4439. [PubMed: 29227476]

Bots M, Kolfschoten IGM, Bres SA, Rademaker MTGA, de Roo GM, Krüse M, Franken KLMC, Hahne M, Froelich CJ, Melief CJM, et al. (2005). SPI-CI and SPI-6 cooperate in the protection from effector cell-mediated cytotoxicity. Blood 105, 1153–1161. 10.1182/blood-2004-03-0791. [PubMed: 15454490]

Bray NL, Pimentel H, Melsted P, and Pachter L (2016). Near-optimal probabilistic RNA-seq quantification. Nat. Biotechnol 34, 525–527. 10.1038/nbt.3519. [PubMed: 27043002]

Buffett RF, Grace JT Jr., DiBerardino LA, and Mirand EA (1969). Vertical transmission of murine leukemia virus through successive generations. Cancer Res. 29, 596–602. [PubMed: 4304387]

Caruso R, Warner N, Inohara N, and Núñez G (2014). NOD1 and NOD2: signaling, host defense, and inflammatory disease. Immunity 41, 898–908. 10.1016/j.immuni.2014.12.010. [PubMed: 25526305]

Case LK, Petell L, Yurkovetskiy L, Purdy A, Savage KJ, and Golovkina TV (2008). Replication of beta- and gammaretroviruses is restricted in I/LnJ mice via the same genetic mechanism. J. Virol 82, 1438–1447, JVI.01991-07 [pii]. 10.1128/JVI.01991-07. [PubMed: 18057254]

Chen GY, Shaw MH, Redondo G, and Núñez G (2008). The innate immune receptor Nod1 protects the intestine from inflammation-induced tumorigenesis. Cancer Res. 68, 10060–10067. 10.1158/0008-5472.Can-08-2061. [PubMed: 19074871]

Chen J, Crispín JC, Dalle Lucca J, and Tsokos GC (2011). A novel inhibitor of the alternative pathway of complement attenuates intestinal ischemia/reperfusion-induced injury. J. Surg. Res 167, e131–136. 10.1016/j.jss.2009.05.041. [PubMed: 19691988]

Chen M, Muckersie E, Luo C, Forrester JV, and Xu H (2010). Inhibition of the alternative pathway of complement activation reduces inflammation in experimental autoimmune uveoretinitis. Eur. J. Immunol 40, 2870–2881. 10.1002/eji.201040323. [PubMed: 20806290]

Chirgwin JM, Przybyla AE, MacDonald RJ, and Rutter WJ (1979). Isolation of biologically active ribonucleic acid from sources enriched in ribonuclease. Biochemistry 18, 5294–5299. [PubMed: 518835]

Crowe NY, Smyth MJ, and Godfrey DI (2002). A critical role for natural killer T cells in immunosurveillance of methylcholanthrene-induced sarcomas. J. Exp. Med 196, 119–127. 10.1084/jem.20020092. [PubMed: 12093876]

Cuffaro B, Assohoun ALW, Boutillier D, Súkeníková L, Desramaut J, Boudebbouze S, Salomé-Desnoulez S, Hrdý J, Waligora-Dupriet AJ, Maguin E, and Grangette C (2020). In vitro characterization of gut microbiota-derived commensal Strains: selection of Parabacteroides distasonis strains alleviating TNBS-induced colitis in mice. Cells 9. 10.3390/cells9092104.

Oliveira-Nascimento L, Massari P, and Wetzler LM (2012). The role of TLR2 in infection and immunity. Front. Immunol 3, 79. 10.3389/fimmu.2012.00079. [PubMed: 22566960]

Dewhirst FE, Chien CC, Paster BJ, Ericson RL, Orcutt RP, Schauer DB, and Fox JG (1999). Phylogeny of the defined murine microbiota: altered Schaedler flora. Appl. Environ. Microbiol 65, 3287–3292. [PubMed: 10427008]

Dittmer U, He H, Messer RJ, Schimmer S, Olbrich ARM, Ohlen C, Greenberg PD, Stromnes IM, Iwashiro M, Sakaguchi S, et al. (2004). Functional impairment of CD8(+) T cells by regulatory T cells during persistent retroviral infection. Immunity 20, 293–303. [PubMed: 15030773]

Dittmer U, Sutter K, Kassiotis G, Zelinskyy G, Bánki Z, Stoiber H, Santiago ML, and Hasenkrug KJ (2019). Friend retrovirus studies reveal complex interactions between intrinsic, innate and adaptive immunity. FEMS Microbiol. Rev 43, 435–456. 10.1093/femsre/fuz012. [PubMed: 31087035]

Donohoe DR, Holley D, Collins LB, Montgomery SA, Whitmore AC, Hillhouse A, Curry KP, Renner SW, Greenwalt A, Ryan EP, et al. (2014). A gnotobiotic mouse model demonstrates that dietary fiber protects against colorectal tumorigenesis in a microbiota- and butyrate-dependent manner. Cancer Discov. 4, 1387–1397. 10.1158/2159-8290.CD-14-0501. [PubMed: 25266735]

Duggan J, Okonta H, and Chakraborty J (2006). Transmission of Moloney murine leukemia virus (ts-1) by breast milk. J. Gen. Virol 87, 2679–2684. 10.1099/vir.0.82015-0. [PubMed: 16894208]

Ezeji JC, Sarikonda DK, Hopperton A, Erkkila HL, Cohen DE, Martinez SP, Cominelli F, Kuwahara T, Dichosa AEK, Good CE, et al. (2021). Parabacteroides distasonis: intriguing aerotolerant gut anaerobe with emerging antimicrobial resistance and pathogenic and probiotic roles in human health. Gut Microb. 13, 1922241. 10.1080/19490976.2021.1922241.

Fletcher CM, Coyne MJ, Bentley DL, Villa OF, and Comstock LE (2007). Phase-variable expression of a family of glycoproteins imparts a dynamic surface to a symbiont in its human intestinal ecosystem. Proc. Natl. Acad. Sci. USA 104, 2413–2418. 10.1073/pnas.0608797104. [PubMed: 17284602]

Fu W, Wojtkiewicz G, Weissleder R, Benoist C, and Mathis D (2012). Early window of diabetes determinism in NOD mice, dependent on the complement receptor CRIg, identified by noninvasive imaging. Nat. Immunol. 13, 361–368. 10.1038/ni.2233. [PubMed: 22366893]

Graveline R, Segura M, Radzioch D, and Gottschalk M (2007). TLR2-dependent recognition of Streptococcus suis is modulated by the presence of capsular polysaccharide which modifies macrophage responsiveness. Int. Immunol 19, 375–389. 10.1093/intimm/dxm003. [PubMed: 17307800]

Grivennikov SI, Greten FR, and Karin M (2010). Immunity, inflammation, and cancer. Cell 140, 883–899. 10.1016/j.cell.2010.01.025. [PubMed: 20303878]

Han SH, Kim JH, Martin M, Michalek SM, and Nahm MH (2003). Pneumococcal lipoteichoic acid (LTA) is not as potent as staphylococcal LTA in stimulating Toll-like receptor 2. Infect. Immun 71, 5541–5548. 10.1128/IAI.71.10.5541-5548.2003. [PubMed: 14500472]

Hasegawa M, Yang K, Hashimoto M, Park J-H, Kim Y-G, Fujimoto Y, Nuñez G, Fukase K, and Inohara N (2006). Differential Release and distribution of Nod1 and Nod2 Immunostimulatory molecules among bacterial species and environments. J. Biol. Chem 281, 29054–29063. 10.1074/jbc.M602638200. [PubMed: 16870615]

Haymaker C, Yang Y, Wang J, Zou Q, Sahoo A, Alekseev A, Singh D, Ritthipichai K, Hailemichael Y, Hoang ON, et al. (2017). Absence of Grail promotes CD8(+) T cell anti-tumour activity. Nat. Commun 8, 239. 10.1038/s41467-017-00252-w. [PubMed: 28798332]

Hicklin DJ, Marincola FM, and Ferrone S (1999). HLA class I antigen down-regulation in human cancers: T-cell immunotherapy revives an old story. Mol. Med. Today 5, 178–186. 10.1016/s1357-4310(99)01451-3. [PubMed: 10203751]

Hook LM, Jude BA, Ter-Grigorov VS, Hartley JW, Morse HC 3rd, Trainin Z, Toder V, Chervonsky AV, and Golovkina TV (2002). Characterization of a novel murine retrovirus mixture that facilitates hematopoiesis. J. Virol 76, 12112–12122. [PubMed: 12414952]

Hope ME, Hold GL, Kain R, and El-Omar EM (2005). Sporadic colorectal cancer–role of the commensal microbiota. FEMS Microbiol. Lett 244, 1–7. 10.1016/j.femsle.2005.01.029. [PubMed: 15727814]

Isaak DD, Bartizal KF, and Caulfield MJ (1988). Decreased pathogenicity of murine leukemia virus-Moloney in gnotobiotic mice. Leukemia 2, 540–544. [PubMed: 3261822]

Jacobs JFM, Nierkens S, Figdor CG, de Vries IJM, and Adema GJ (2012). Regulatory T cells in melanoma: the final hurdle towards effective immunotherapy? Lancet Oncol. 13, e32–42. 10.1016/S1470-2045(11)70155-3. [PubMed: 22225723]

Jacobson AN, Choudhury BP, and Fischbach MA (2018). The biosynthesis of Lipooligosaccharide from Bacteroides thetaiotaomicron. mBio 9, e02289–17. 10.1128/mBio.02289-17. [PubMed: 29535205]

Jiang L, Wang YJ, Zhao J, Uehara M, Hou Q, Kasinath V, Ichimura T, Banouni N, Dai L, Li X, et al. (2020). Direct tumor killing and immunotherapy through anti-SerpinB9 therapy. Cell 183, 1219–1233.e18. 10.1016/j.cell.2020.10.045. [PubMed: 33242418]

Johnsen AK, Templeton DJ, Sy M, and Harding CV (1999). Deficiency of transporter for antigen presentation (TAP) in tumor cells allows evasion of immune surveillance and increases tumorigenesis. J. Immunol 163, 4224–4231. [PubMed: 10510359]

Kane M, Case LK, Kopaskie K, Kozlova A, MacDearmid C, Chervonsky AV, and Golovkina TV (2011). Successful transmission of a retrovirus depends on the commensal microbiota. Science 334, 245–249. 10.1126/science.1210718. [PubMed: 21998394]

Karo JM, Schatz DG, and Sun JC (2014). The RAG recombinase dictates functional heterogeneity and cellular fitness in natural killer cells. Cell 159, 94–107. 10.1016/j.cell.2014.08.026. [PubMed: 25259923]

Kim R, Emi M, and Tanabe K (2007). Cancer immunoediting from immune surveillance to immune escape. Immunology 121, 1–14. 10.1111/j.1365-2567.2007.02587.x. [PubMed: 17386080]

Kim S, Covington A, and Pamer EG (2017). The intestinal microbiota: antibiotics, colonization resistance, and enteric pathogens. Immunol. Rev 279, 90–105. 10.1111/imr.12563. [PubMed: 28856737]

Kinzler KW, and Vogelstein B (1996). Lessons from hereditary colorectal cancer. Cell 87, 159–170. [PubMed: 8861899]

Kouttab NM, and Jutila JW (1972). Friend leukemia virus infection in germfree mice following antigen stimulation. J. Immunol 108, 591–595. [PubMed: 4551850]

Kriegel MA, Rathinam C, and Flavell RA (2009). E3 ubiquitin ligase GRAIL controls primary T cell activation and oral tolerance. Proc. Natl. Acad. Sci. USA 106, 16770–16775. 10.1073/pnas.0908957106. [PubMed: 19805371]

Kuss SK, Best GT, Etheredge CA, Pruijssers AJ, Frierson JM, Hooper LV, Dermody TS, and Pfeiffer JK (2011). Intestinal microbiota promote enteric virus replication and systemic pathogenesis. Science 334, 249–252. [PubMed: 21998395]

Kverka M, Zakostelska Z, Klimesova K, Sokol D, Hudcovic T, Hrncir T, Rossmann P, Mrazek J, Kopecny J, Verdu EF, and Tlaskalova-Hogenova H (2011). Oral administration of Parabacteroides distasonis antigens attenuates experimental murine colitis through modulation of immunity and microbiota composition. Clin. Exp. Immunol 163, 250–259. 10.1111/j.1365-2249.2010.04286.x. [PubMed: 21087444]

Lee J, Tattoli I, Wojtal KA, Vavricka SR, Philpott DJ, and Girardin SE (2009). pH-dependent internalization of muramyl peptides from early endosomes enables Nod1 and Nod2 signaling. J. Biol. Chem 284, 23818–23829. 10.1074/jbc.M109.033670. [PubMed: 19570976]

Lind MH, Rozell B, Wallin RPA, van Hogerlinden M, Ljunggren HG, Toftgård R, and Sur I (2004). Tumor necrosis factor receptor 1-mediated signaling is required for skin cancer development induced by NF-kappaB inhibition. Proc. Natl. Acad. Sci. USA 101, 4972–4977. 10.1073/pnas.0307106101. [PubMed: 15044707]

Lineberry NB, Su LL, Lin JT, Coffey GP, Seroogy CM, and Fathman CG (2008). Cutting edge: the transmembrane E3 ligase GRAIL ubiquitinates the costimulatory molecule CD40 ligand during the induction of T cell anergy. J. Immunol 181, 1622–1626. 10.4049/jimmunol.181.3.1622. [PubMed: 18641297]

Lippitz BE (2013). Cytokine patterns in patients with cancer: a systematic review. Lancet Oncol. 14, e218–228. 10.1016/s1470-2045(12)70582-x. [PubMed: 23639322]

Littman DR, and Pamer EG (2011). Role of the commensal microbiota in normal and pathogenic host immune responses. Cell Host Microbe 10, 311–323. 10.1016/j.chom.2011.10.004. [PubMed: 22018232]

Ma J, Chen J, Bo S, Lu X, and Zhang J (2015). Protective effect of carnosine after chronic cerebral hypoperfusion possibly through suppressing astrocyte activation. Am. J. Transl. Res 7, 2706–2715. [PubMed: 26885268]

Medema JP, de Jong J, Peltenburg LT, Verdegaal EM, Gorter A, Bres SA, Franken KL, Hahne M, Albar JP, Melief CJ, and Offringa R (2001). Blockade of the granzyme B/perforin pathway through overexpression of the serine protease inhibitor PI-9/SPI-6 constitutes a mechanism

for immune escape by tumors. Proc. Natl. Acad. Sci. USA 98, 11515–11520. 10.1073/pnas.201398198. [PubMed: 11562487]

Medzhitov R. (2008). Origin and physiological roles of inflammation. Nature 454, 428–435, nature07201 [pii]. 10.1038/nature07201. [PubMed: 18650913]

Meisel M, Hinterleitner R, Pacis A, Chen L, Earley ZM, Mayassi T, Pierre JF, Ernest JD, Galipeau HJ, Thuille N, et al. (2018). Microbial signals drive pre-leukaemic myeloproliferation in a Tet2-deficient host. Nature 557, 580–584. 10.1038/s41586-018-0125-z. [PubMed: 29769727]

Metelitsa LS, Naidenko OV, Kant A, Wu HW, Loza MJ, Perussia B, Kronenberg M, and Seeger RC (2001). Human NKT cells mediate antitumor cytotoxicity directly by recognizing target cell CD1d with bound ligand or indirectly by producing IL-2 to activate NK cells. J. Immunol 167, 3114–3122. 10.4049/jimmunol.167.6.3114. [PubMed: 11544296]

Mirand EA, and Grace JT Jr. (1963). Responses of germ-free mice to friend virus. Nature 200, 92–93. [PubMed: 14074649]

Nagata S, and Golstein P (1995). The Fas death factor. Science 267, 1449–1456. 10.1126/science.7533326. [PubMed: 7533326]

Nurieva RI, Zheng S, Jin W, Chung Y, Zhang Y, Martinez GJ, Reynolds JM, Wang SL, Lin X, Sun SC, et al. (2010). The E3 ubiquitin ligase GRAIL regulates T cell tolerance and regulatory T cell function by mediating T cell receptor-CD3 degradation. Immunity 32, 670–680. 10.1016/j.immuni.2010.05.002. [PubMed: 20493730]

Pasche B. (2001). Role of transforming growth factor beta in cancer. J. Cell. Physiol 186, 153–168. 10.1002/1097-4652(200002)186:2<153::AID-JCP1016>3.0.CO;2-J. [PubMed: 11169452]

Poltorak A, He X, Smirnova I, Liu M-Y, Van Huffel C, Du X, Birdwell D, Alejos E, Silva M, Galanos C, et al. (1998). Defective LPS signaling in C3H/HeJ and C57BL/10ScCr mice: mutations in *Tlr4* gene. Science 282, 2085–2088. 10.1126/science.282.5396.2085. [PubMed: 9851930]

Quezada SA, Simpson TR, Peggs KS, Merghoub T, Vider J, Fan X, Blasberg R, Yagita H, Muranski P, Antony PA, et al. (2010). Tumor-reactive CD4(+) T cells develop cytotoxic activity and eradicate large established melanoma after transfer into lymphopenic hosts. J. Exp. Med 207, 637–650. 10.1084/jem.20091918. [PubMed: 20156971]

Rakoff-Nahoum S, and Medzhitov R (2007). Regulation of spontaneous intestinal tumorigenesis through the adaptor protein MyD88. Science 317, 124–127. 10.1126/science.1140488. [PubMed: 17615359]

Raskov H, Orhan A, Christensen JP, and Gögenur I (2021). Cytotoxic CD8+ T cells in cancer and cancer immunotherapy. Br. J. Cancer 124, 359–367. 10.1038/s41416-020-01048-4. [PubMed: 32929195]

Reddy BS, Narisawa T, Wright P, Vukusich D, Weisburger JH, and Wynder EL (1975). Colon carcinogenesis with azoxymethane and dimethylhydrazine in germ-free rats. Cancer Res. 35, 287–290. [PubMed: 162868]

Robertson SJ, Ammann CG, Messer RJ, Carmody AB, Myers L, Dittmer U, Nair S, Gerlach N, Evans LH, Cafruny WA, and Hasenkrug KJ (2008). Suppression of acute anti-friend virus CD8+ T-cell responses by coinfection with lactate dehydrogenase-elevating virus. J. Virol 82, 408–418. 10.1128/jvi.01413-07. [PubMed: 17959678]

Robertson SJ, Messer RJ, Carmody AB, and Hasenkrug KJ (2006). In vitro suppression of CD8+ T cell function by Friend virus-induced regulatory T cells. J. Immunol 176, 3342–3349. [PubMed: 16517701]

Rowe WP, Pugh WE, and Hartley JW (1970). Plaque assay techniques for murine leukemia viruses. Virology 42, 1136–1139. [PubMed: 4099080]

Samuelson J. (1999). Why metronidazole is active against both bacteria and parasites. Antimicrob. Agents Chemother 43, 1533–1541. 10.1128/AAC.43.7.1533. [PubMed: 10390199]

Sarma-Rupavtarm RB, Ge Z, Schauer DB, Fox JG, and Polz MF (2004). Spatial distribution and stability of the eight microbial species of the altered schaedler flora in the mouse gastrointestinal tract. Appl. Environ. Microbiol 70, 2791–2800. [PubMed: 15128534]

Shankaran V, Ikeda H, Bruce AT, White JM, Swanson PE, Old LJ, and Schreiber RD (2001). IFNgamma and lymphocytes prevent primary tumour development and shape tumour immunogenicity. Nature 410, 1107–1111. 10.1038/35074122. [PubMed: 11323675]

Sivan A, Corrales L, Hubert N, Williams JB, Aquino-Michaels K, Earley ZM, Benyamin FW, Lei YM, Jabri B, Alegre ML, et al. (2015). Commensal Bifidobacterium promotes antitumor immunity and facilitates anti-PD-L1 efficacy. Science 350, 1084–1089. 10.1126/science.aac4255. [PubMed: 26541606]

Sleytr UB, Messner P, Pum D, and Sára M (1993). Crystalline bacterial cell surface layers. Mol. Microbiol 10, 911–916. 10.1111/j.1365-2958.1993.tb00962.x. [PubMed: 7934867]

ten Berge RL, Meijer CJLM, Dukers DF, Kummer JA, Bladergroen BA, Vos W, Hack CE, Ossenkoppele GJ, and Oudejans JJ (2002). Expression levels of apoptosis-related proteins predict clinical outcome in anaplastic large cell lymphoma. Blood 99, 4540–4546. 10.1182/blood.v99.12.4540. [PubMed: 12036886]

Ter-Grigorov VS, Krifuks O, Liubashevsky E, Nyska A, Trainin Z, and Toder V (1997). A new transmissible AIDS-like disease in mice induced by alloimmune stimuli. Nat. Med 3, 37–41. [PubMed: 8986738]

Toes RE, Ossendorp F, Offringa R, and Melief CJ (1999). CD4 T cells and their role in antitumor immune responses. J. Exp. Med 189, 753–756. 10.1084/jem.189.5.753. [PubMed: 10049938]

Uchiyama R, Chassaing B, Zhang B, and Gewirtz AT (2014). Antibiotic treatment suppresses rotavirus infection and enhances specific humoral immunity. J. Infect. Dis 210, 171–182. 10.1093/infdis/jiu037. [PubMed: 24436449]

Uhlen M, Zhang C, Lee S, Sjöstedt E, Fagerberg L, Bidkhori G, Benfeitas R, Arif M, Liu Z, Edfors F, et al. (2017). A pathology atlas of the human cancer transcriptome. Science 357, eaan2507. 10.1126/science.aan2507. [PubMed: 28818916]

Vétizou M, Pitt JM, Daillère R, Lepage P, Waldschmitt N, Flament C, Rusakiewicz S, Routy B, Roberti MP, Duong CPM, et al. (2015). Anti-cancer immunotherapy by CTLA-4 blockade relies on the gut microbiota. Science 350, 1079–1084. 10.1126/science.aad1329. [PubMed: 26541610]

Vinay DS, Ryan EP, Pawelec G, Talib WH, Stagg J, Elkord E, Lichtor T, Decker WK, Whelan RL, Kumara HMCS, et al. (2015). Immune evasion in cancer: mechanistic basis and therapeutic strategies. Semin. Cancer Biol 35 (Suppl), S185–S198. 10.1016/j.semcancer.2015.03.004. [PubMed: 25818339]

Vogt L, Schmitz N, Kurrer MO, Bauer M, Hinton HI, Behnke S, Gatto D, Sebbel P, Beerli RR, Sonderegger I, et al. (2006). VSIG4, a B7 family-related protein, is a negative regulator of T cell activation. J. Clin. Invest 116, 2817–2826. 10.1172/JCI25673. [PubMed: 17016562]

Wilks J, Beilinson H, Theriault B, Chervonsky A, and Golovkina T (2014). Antibody-mediated immune control of a retrovirus does not require the microbiota. J. Virol 88, 6524–6527. 10.1128/JVI.00251-14. [PubMed: 24648456]

Wilks J, Lien E, Jacobson AN, Fischbach MA, Qureshi N, Chervonsky AV, and Golovkina TV (2015). Mammalian lipopolysaccharide receptors incorporated into the retroviral envelope augment virus transmission. Cell Host Microbe 18, 456–462. 10.1016/j.chom.2015.09.005. [PubMed: 26468748]

Xie Y, Akpinarli A, Maris C, Hipkiss EL, Lane M, Kwon E-KM, Muranski P, Restifo NP, and Antony PA (2010). Naive tumor-specific CD4+ T cells differentiated in vivo eradicate established melanoma. J. Exp. Med 207, 651–667. 10.1084/jem.20091921. [PubMed: 20156973]

Xu S, Sun Z, Li L, Liu J, He J, Song D, Shan G, Liu H, and Wu X (2010). Induction of T cells suppression by dendritic cells transfected with VSIG4 recombinant adenovirus. Immunol. Lett 128, 46–50. 10.1016/j.imlet.2009.11.003. [PubMed: 19914289]

Yoshimoto S, Loo TM, Atarashi K, Kanda H, Sato S, Oyadomari S, Iwakura Y, Oshima K, Morita H, Hattori M, et al. (2013). Obesity-induced gut microbial metabolite promotes liver cancer through senescence secretome. Nature 499, 97–101. 10.1038/nature12347. [PubMed: 23803760]

Young GR, Eksmond U, Salcedo R, Alexopoulou L, Stoye JP, and Kassiotis G (2012). Resurrection of endogenous retroviruses in antibody-deficient mice. Nature 491, 774–778. 10.1038/nature11599. [PubMed: 23103862]

Zeng Z, Surewaard BGJ, Wong CHY, Geoghegan JA, Jenne CN, and Kubes P (2016). CRIg functions as a macrophage pattern recognition receptor to directly bind and capture blood-borne gram-positive bacteria. Cell Host Microbe 20, 99–106. 10.1016/j.chom.2016.06.002. [PubMed: 27345697]

Zhang J, Socolovsky M, Gross AW, and Lodish HF (2003). Role of Ras signaling in erythroid differentiation of mouse fetal liver cells: functional analysis by a flow cytometry-based novel culture system. Blood 102, 3938–3946. 10.1182/blood-2003-05-1479. [PubMed: 12907435]

Highlights

- Retroviral pathogenesis is promoted by gut commensal bacteria
- Commensal bacteria suppress the adaptive immune response
- Suppression is mediated by negative immune regulators Rnf128 and Serpinb9b
- Rnf128 and Serpinb9b are drivers of virally induced tumorigenesis

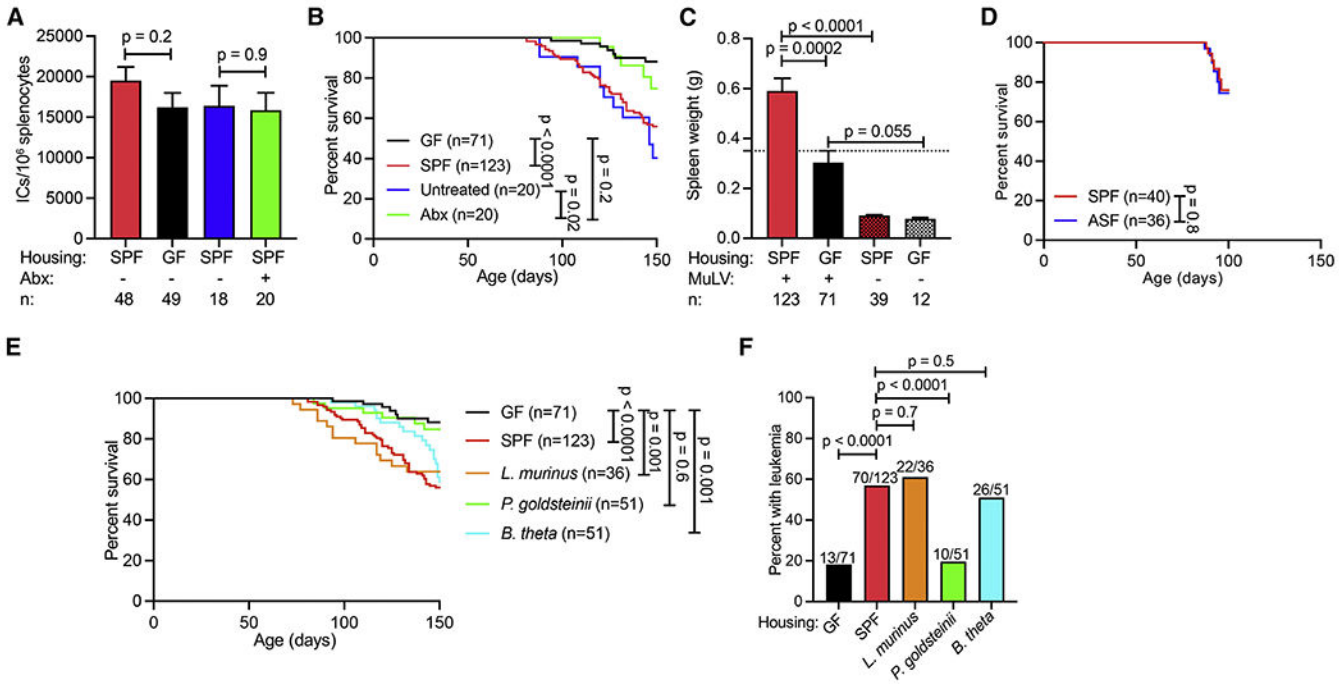

Figure 1. Dependence of MuLV-induced leukemia development on commensal bacteria

Adult BALB/cJ females from different experimental groups were injected with MuLV and bred (G0 mice). Their offspring (G1 mice) were monitored for leukemia. Diseased mice removed from the cohorts and mice surviving up to 150 days were examined according to a leukemia scoring system based on histological analysis of the spleen (Figure S1C).

(A) Comparison of viral load (number of infectious centers [ICs]) in preleukemic SPF-, GF-, and Abx-treated animals with score 1.

(B) Survival curves of G1 mice from the same groups.

(C) Spleen weights of infected and uninfected SPF and GF mice at age 4–5 months. Dotted horizontal line indicates 0.35 g (all mice with spleen weight ≥ 0.35 g have leukemia, Figures S1D–S1F).

(D) Survival curves of MuLV-infected SPF- and ASF-colonized BALB/cJ mice observed for 97 days.

(E) Survival of GF, SPF, and gnotobiotic BALB/cJ mice colonized with single bacterial lineages monitored for 150 days.

(F) Final assessment of leukemia development in mice from these groups at day 150. Abx, antibiotic. n, number of mice used per group.

p values were calculated using an unpaired t test (A and C), Fisher's exact test (F) and Mantel-Cox test (B, D, and E). Error bars indicate standard error of the mean.

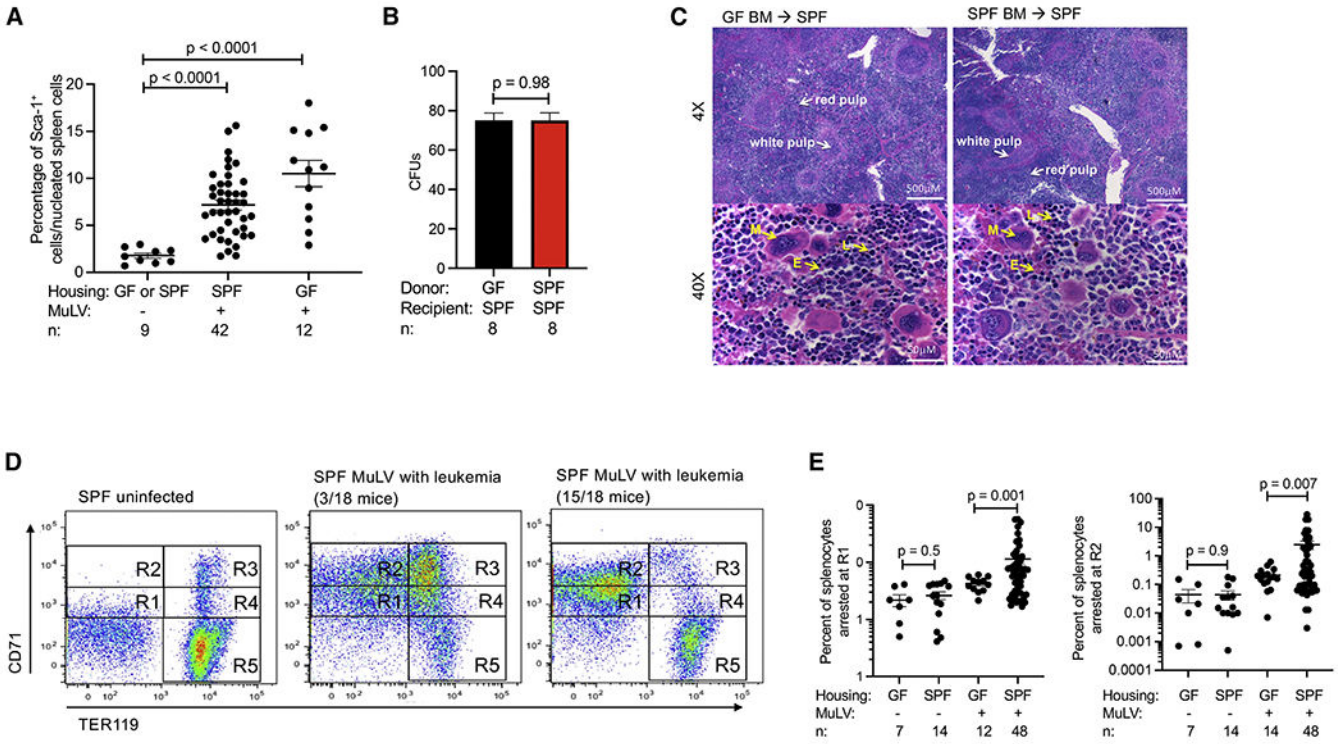

Figure 2. Comparison of leukemia development in SPF and GF BALB/c mice

(A) Increase in extramedullary hematopoiesis in the spleens of infected mice. Nucleated splenocytes were stained with anti-mouse Sca-1 mAb and analyzed by FACS. Uninfected GF and SPF BALB/cJ mice were used as negative controls.

(B and C) Frequency of HSCs in the bone marrow (BM) of GF and SPF mice measured by colony formation in the spleens of lethally irradiated SPF BALB/cJ recipients. Splenic colonies were counted 9 days after transfer of 2×10^6 BM cells. CFUs, colony forming units per 2×10^6 BM cells. n, number of recipients. Combined data from two independent experiments (B). Fixed spleens were sectioned and stained with hematoxylin and eosin to visualize differentiated cells within colonies. Representative images of one of five recipient mice per group. Red and white pulp indicated by white arrows. Cells of the different hematopoietic lineages are identified by yellow arrows. M, megakaryocyte; E, erythroid precursor; L, lymphocyte (C).

(D) Determination of a specific developmental stage at which erythroid cells are stalled in infected SPF mice. The stages of erythrocyte development from the megakaryocyte-erythrocyte progenitor stage to the final red blood cell stage (R1-R5) were determined as described (Zhang et al., 2003) by staining nucleated spleen cells with a mixture of anti-mouse CD71/anti-mouse Ter119 mAbs. R1 corresponds to erythroid burst-forming units and erythroid colony forming units; R2 corresponds to proerythroblasts and basophilic erythroblasts; R3 is made up of early and late basophilic erythroblasts; R4 corresponds to polychromatophilic and orthochromatophilic erythroblasts and R5 contains reticulocytes and erythrocytes. Staining profiles of splenocytes from the indicated mice. Of the 18 SPF leukemic mice analyzed, 15/18 mice exhibited $CD71^{high}TER19^{low}$ leukemias and 3/18 mice exhibited $CD71^{high}TER19^{high}$ leukemias.

(E) A quantitative comparison of cell numbers arrested at R1 (left) and R2 (right) see (D) stage in SPF and GF mice. n, number of mice used. p values calculated using unpaired t test. Error bars indicate standard error of the mean.

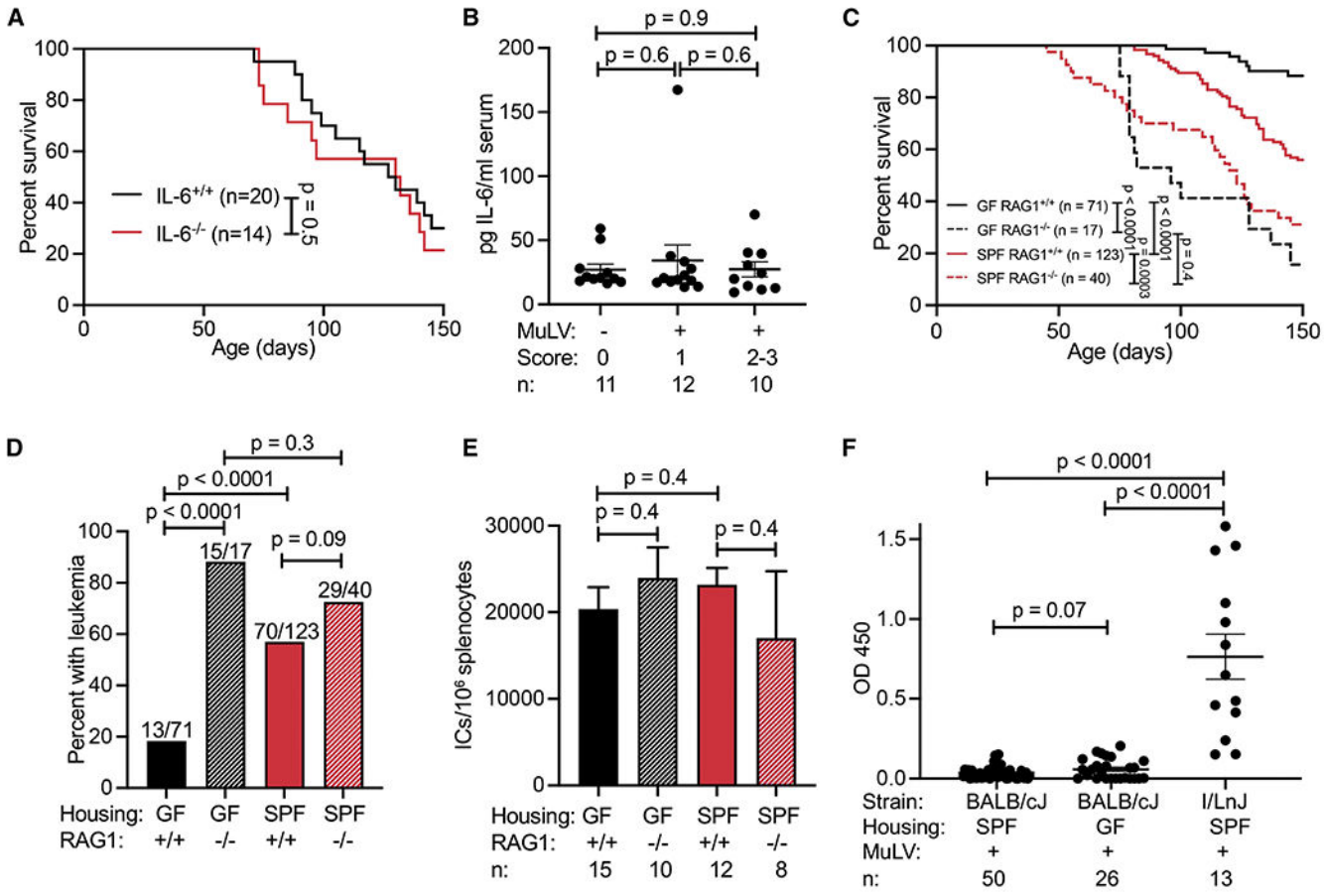

Figure 3. Comparison of leukemia susceptibility of immunosufficient- and immunodeficient-infected GF and SPF BALB/cJ mice

(A) Survival of IL-6-sufficient and IL-6-deficient MuLV-infected SPF BALB/cJ mice.

(B) Serum cytokine concentration of IL-6 was measured in uninfected (score 0), infected preleukemic (score 1), and infected leukemic (scores 2–3) BALB/cJ mice using a flow cytometry bead-based assay.

(C) Survival of infected RAG1-sufficient SPF, RAG1-deficient SPF, RAG1-sufficient GF, and RAG1-deficient GF BALB/cJ mice during 150 days.

(D) Total leukemia incidence of infected indicated mice at 150 days.

(E) Comparison of the viral burden (frequency of infected cells per 10^6 splenocytes) in indicated preleukemic mice (score 1).

(F) MuLV-specific ELISA to detect anti-virus antibodies. I/LnJ mice fostered on MuLV-infected BALB/cJ females are included as a positive control as they produce virus-neutralizing antibodies (Case et al., 2008). n, number of mice used.

p values calculated using Mantel-Cox test (A and C), Fisher's exact test (D), or unpaired t test (B, E, and F). Error bars indicate standard error of the mean.

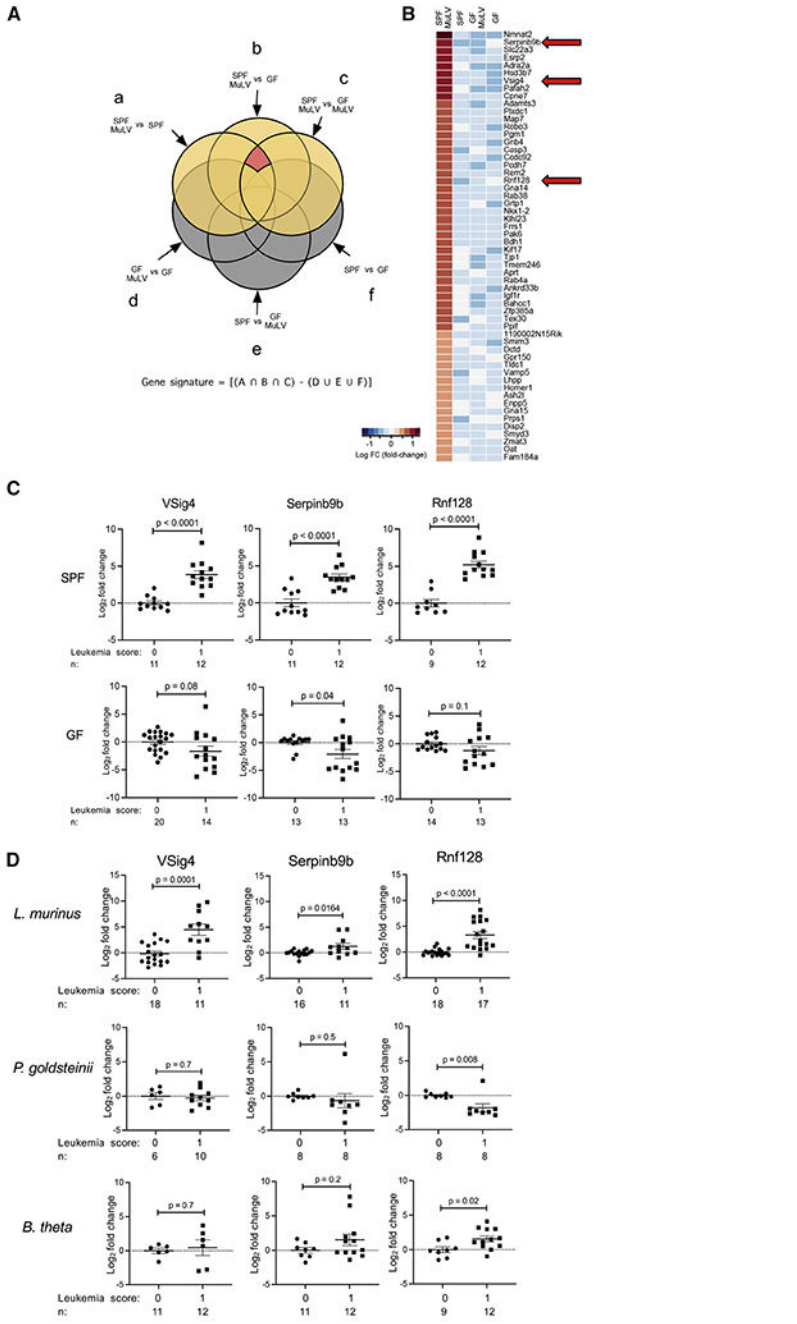

Figure 4. Induction of negative regulators of the immune response by commensal bacteria and the virus

RNA isolated from spleens of preleukemic mice (score 1) of four groups (SPF ± MuLV infection and GF ± MuLV infection) was subjected to high-throughput sequencing.

(A) Diagram detailing the series of operations taken to identify genes differentially expressed in spleens of mice from four groups. See explanation in the text.

(B) Heatmap of gene expression found to be significantly upregulated in SPF MuLV-infected mice compared with mice from all other groups. Red arrows indicate established negative regulators of adaptive immunity.

(C) Real-time quantitative PCR (qPCR) measurement of expression of the negative regulators of immune response in SPF and GF mice. Mice were either uninfected (score 0) or infected pre-leukemic (score 1). n, number of mice used.

(D) qPCR with RNA isolated from spleens of uninfected (score 0) and infected pre-leukemic (score 1) mice colonized with *L. murinus*, *P. goldsteinii*, or *B. theta*. Data are represented as $\log_2$ fold change compared with uninfected controls, normalized to the endogenous control (β-actin).

Two-way ANOVA was used to identify genes upregulated in infected SPF mice compared with uninfected SPF, uninfected GF, and infected GF mice (A and B). p values calculated using unpaired t test (C and D). Error bars indicate standard error of the mean.

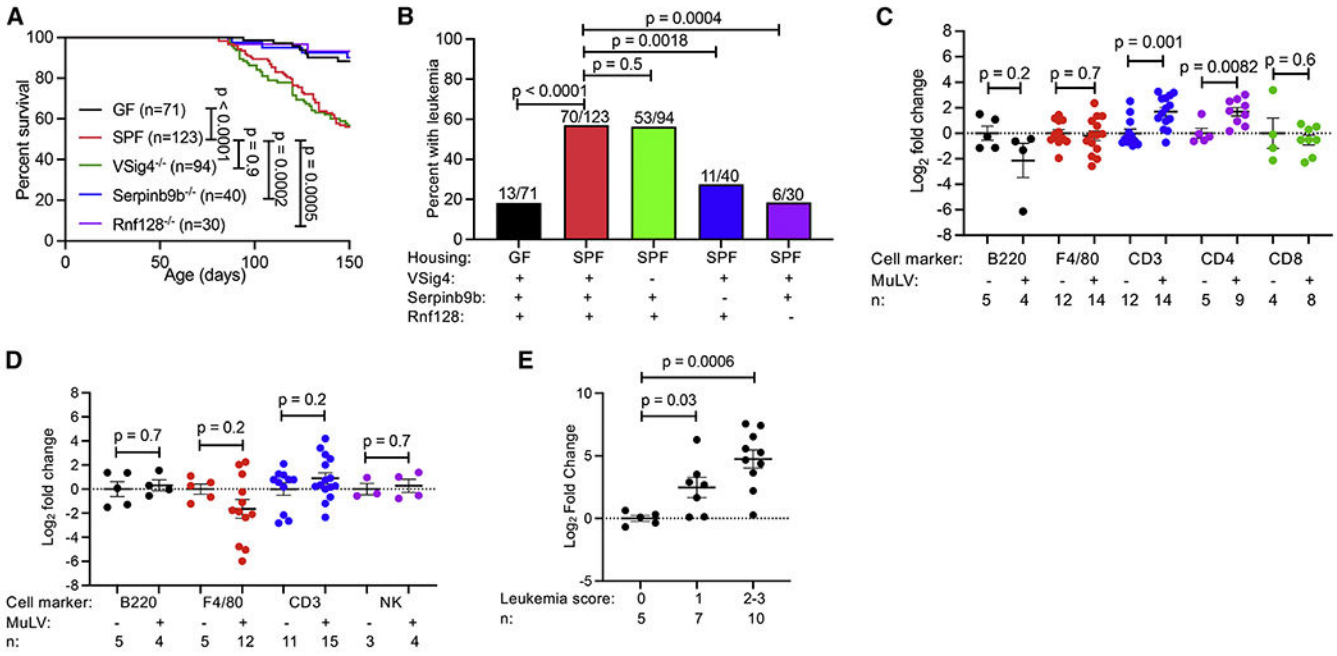

Figure 5. Resistance of Rnf128-deficient and Serpinb9b-deficient SPF mice to MuLV-induced leukemia

MuLV-infected BALB/cJ mice deficient in VSig4, Serpinb9b, or Rnf128 were monitored for leukemia development.

(A) Survival curves for up to 150 days are shown.

(B) Final leukemia assessment at 150 days.

(C and D) Expression of Rnf128 (C) or Serpinb9b (D) in the MACS sorted splenocytes from WT uninfected and infected mice analyzed by qPCR.

(E) Serpinb9b expression in RNA isolated from spleens of SPF RAG1$^{-/-}$ uninfected (score 0), pre-leukemic (score 1), and leukemic (scores 2–3) mice analyzed via qPCR. qPCR data are represented as $\log_2$ fold change compared with uninfected controls and normalized to the endogenous control β-actin. n, number of mice used.

p values calculated using Mantel-Cox test (A), Fisher's exact test (B), or unpaired t test (C–E). Error bars indicate standard error of the mean.

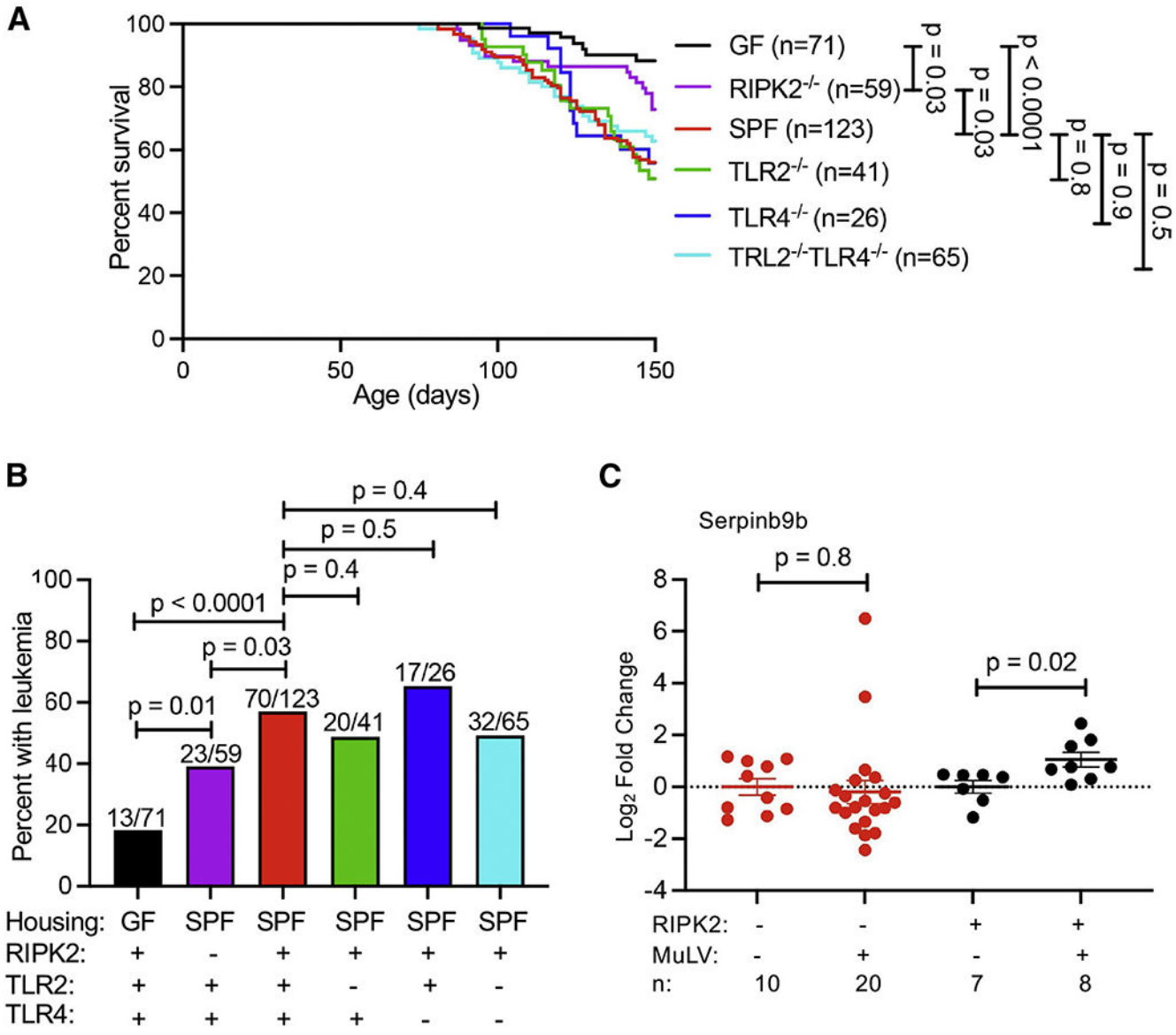

Figure 6. NOD1/2 adaptor RIPK2 contributes to MuLV-induced leukemia via upregulation of Serpinb9b

Leukemia development was monitored in RLMuLV-infected SPF BALB/cJ mice deficient in either TLR2, TLR4, TLR2/TLR4, or RIPK2.

(A) Survival curves up to 150 days.

(B) Total leukemia incidence at 150 days.

(C) Expression of Serpinb9b in splenic RNA from RIPK2$^{-/-}$ and control RIPK2$^{+/-}$ uninfected and infected mice analyzed by qPCR. Data are represented as $\log_2$ fold change compared with uninfected controls, normalized to the endogenous control (β-actin). n, number of mice used. Error bars indicate standard error of the mean.

p values calculated using Mantel-Cox test (A), Fisher's exact test (B) or unpaired t test (C).

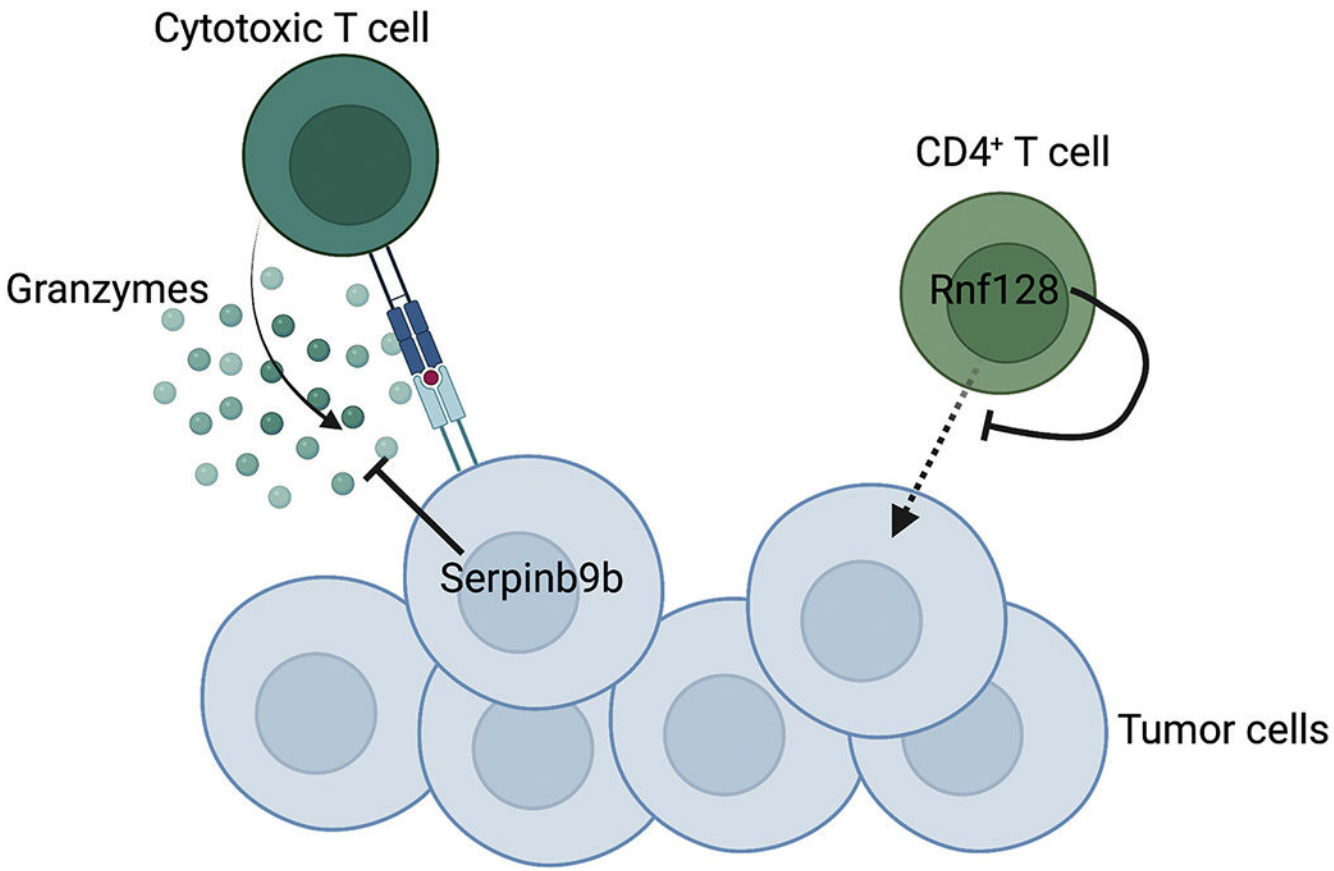

Figure 7. Hypothetical model of Serpinb9b- and Rnf128-mediated suppression of the adaptive immune response

Upregulation of Serpinb9b, likely in tumor cells, potentially promotes tumor development through inactivation of cytotoxic granzymes. Rnf128 upregulation in $CD4^+$ T cells stimulates unresponsiveness, inhibiting their immune function.